



# Two leg voltage source converter for voltage and frequency control in wind power Generation



**A Project Report**

*Submitted by*

**K.Gurumoorthi - 0920105004**

*in partial fulfillment for the award of the degree*

of

**Master of Engineering**

in

**Power Electronics and Drives**

**DEPARTMENT OF ELECTRICAL & ELECTRONICS  
ENGINEERING**

**KUMARAGURU COLLEGE OF TECHNOLOGY  
COIMBATORE – 641 049**

(An Autonomous Institution Affiliated to Anna University, Coimbatore.)

ANNA UNIVERSITY OF TECHNOLOGY: COIMBATORE

**APRIL 2011**

# ANNA UNIVERSITY: COIMBATORE

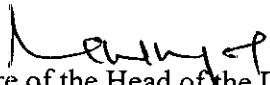
## BONAFIDE CERTIFICATE

Certified that this project report entitled “Two leg voltage source converter for voltage and frequency control in wind power generation” is the bonafide work of

K.Gurumoorthi

Register No.0920105004

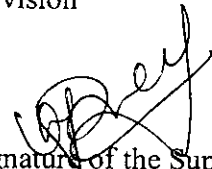
Who carried out the project work under my Supervision



Signature of the Head of the Department

Dr. Rani Thottungal

HOD / EEE

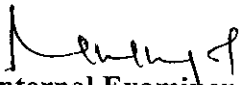


Signature of the Supervisor

Mrs.K.Premalatha

Asst.Proffessor

Certified that the candidate with university Register No. 0920105004 was examined in project viva voce Examination held on 26-04-2011



Internal Examiner



External Examiner

DEPARTMENT OF ELECTRICAL & ELECTRONICS ENGINEERING  
KUMARAGURU COLLEGE OF TECHNOLOGY, COIMBATORE 641 006

(An Autonomous Institution Affiliated to Anna University, Coimbatore.) **PROOF**  
**OF PUBLICATION**



institute of engineering

Sathy road, Kovilpalayam, Coimbatore- 641 107

DEPARTMENT OF ELECTRICAL AND ELECTRONICS ENGINEERING

**CSIR**

Sponsored

FIRST NATIONAL CONFERENCE

On

**“Recent Advances in Power Electronics and Industrial Drives”**

Certificate of Attendance

It is hereby certified that K. GURUMOORTHY  
representing KUMARAGURU COLLEGE OF TECHNOLOGY COIMBATORE  
has participated in the First National Conference on **“RECENT ADVANCES  
IN POWER ELECTRONICS AND INDUSTRIAL DRIVES”** (PEID) 2011  
and presented a paper titled TWO LEG VOLTAGE SOURCE CONVERTER  
FOR VOLTAGE AND FREQUENCY CONTROL IN on March 04/05,2011  
WIND POWER GENERATION

A handwritten signature in black ink, appearing to read "A. Nirmal Kumar".

**Dr.A.Nirmal Kumar**  
CONVENER

A handwritten signature in black ink, appearing to read "Chitra Manohar".

**Dr.Chitra Manohar**  
PATRON

## ABSTRACT

This project deals with the  $I \cdot \cos\phi$  algorithm for the voltage and frequency control (VFC) of an autonomous wind power generation using an isolated asynchronous generator (IAG) feeding three-phase loads. The reference source currents are estimated using the  $I \cdot \cos\phi$  algorithm to control the voltage and frequency of IAG system. Two-leg voltage source converter (VSC) with split capacitor and an isolation connected transformer is used as an integrated VSC. The reduced switch integrated VSC with a battery energy storage system (BESS) is used for the power management of the wind energy conversion system (WECS). The WECS is modeled and simulated in the MATLAB using the Simulink and the sim power system (SPS) toolboxes. Bi-directional power flow capabilities of the proposed voltage and frequency (VF) controller in WECS are demonstrated through simulation results. The proposed voltage and frequency(VF) controller functions as a voltage regulator, a load leveler in the wind energy conversion system.

## ACKNOWLEDGEMENT

At this delightful moment of having accomplished, I extend my sincere thanks to the management of Kumaraguru College of Technology.

I am greatly indebted to our principal **Dr. S. Ramachandran** for his permission to do this project and for providing me necessary facilities for completing my project in our institution.

I am permanently indebted and convey my deep gratitude to the HOD of Electrical and Electronics Engineering, **Dr. Rani Thottungal** for giving me valuable guidance throughout this project and technical advice during the moment of hardships.

I am deeply indebted to my guide **Mrs. K.Premalatha** Assistant Professor, Electrical and Electronics Engineering Department who has inspired to do this project and gave me valuable technical guidance, timely suggestions and providing me the necessary facilities, which went a long way towards successful completion of this project.

I am also thankful to my **Teaching and Non-Teaching staffs** of Electrical and Electronics Engineering department, for their kind help and encouragement.

Last but not least, I extend my sincere thanks to my **Parents and Friends** who have contributed their ideas and encouraged me for completing this project.

# CONTENTS

<b>TITLE</b>	<b>Page No</b>
BONAFIDE CERTIFICATE	ii
PROOF OF PUBLICATION	iii
ABSTRACT	iv
ACKNOWLEDGEMENT	v
CONTENTS	vi
LIST OF FIGURES	viii
ABBREVIATIONS	ix
<b>1. INTRODUCTION</b>	
1.1 Introduction	2
1.2 Objectives of the project	4
1.3 Organization of the thesis	5
<b>2. METHODOLOGY</b>	
2.1 Existing three leg converter	7
2.2 Simulation output	8
2.2.1 Constant output voltage	
2.2.2 Constant output frequency	
2.3 Proposed two leg Converter	10
<b>3. MODELLING OF PROPOSED CONTROLLER</b>	
3.1 Controller for two leg converter	13
3.1.1 Computation of phase voltage	
3.1.2 Computation inphase and quadrature unit templates	
3.1.3 Computation of source frequency	
3.1.4 Estimation of fundamental reference real power	
3.1.5 Extraction of amplitude of fundamental reactive power of load currents	
3.1.6 Estimation of fundamental reference real power of source currents	
3.1.7 Estimation of fundamental reference reactive power of source currents	

3.1.8 Estimation of fundamental power component of reference source currents	
3.1.9 PWM Generator	
3.2 Modeling of the mechanical system	18
3.3 Modeling of the VFC	19
<b>4. SIMULATION</b>	
4.1 MATLAB	22
4.2 Simulation models	23
4.2.1 Simulation diagram of standalone wind power generation	
4.2. Control Circuit of Proposed Power Converter	
4.3 Simulation results	26
4.4 Parameters	26
4.5 Output voltage	26
4.6 Output frequency	27
4.7 Output current	27
<b>5. HARDWARE IMPLEMENTATION</b>	
5.1 Block diagram	29
5.2 Two leg voltage source converter circuit with load	30
5.3 Microcontroller	31
5.4 Power Supply for the Microcontroller	32
5.5 Photograph of hardware	33
5.6 Hardware testing and results	34
<b>6. CONCLUSION</b>	
6.1 Conclusion	37
<b>REFERENCES</b>	38
<b>APPENDIX I</b>	39

## LIST OF FIGURES

Figure No.	Title	Page No.
2.1	Standalone alone induction generator with three leg voltage source converter	7
2.2	Constant output voltage	9
2.3	Constant output frequency	9
2.4	Block diagram of proposed two leg VFC in standalone wind power system	10
2.5	Circuit diagram of two leg converter in standalone wind power generation	11
3.1	Controller block diagram of two leg converter	14
3.2	Control algorithm block digram	19
4.1	Simulation Diagram of Proposed Power Converter	23
4.2	Icos $\Phi$ algorithm simulation diagram	24
4.3	Control Circuit of Proposed Power Converter	25
4.4	Constant output voltage of proposed system	26
4.5	Constant output frequency of proposed system	27
4.6	Constant output voltage of proposed system	27
5.1	Block Diagram of Prototype	29
5.2	Two leg voltage source converter circuit with load	30
5.3	Schematic of Microcontroller circuit	31
5.4	Power Supply Block Diagram	32
5.5	Power supply for Microcontroller	32
5.6	Hardware photograph	33
5.7	Output voltage waveform	34
5.8	PWM signal for two leg converter	34
5.9	Battery charging waveform	35
5.10	Battery discharging waveform	36

## **ABBREVIATIONS**

WECS	-	Wind Energy Conversion System
IAG	-	Isolated Asynchronous Generator
PWM	-	Pulse Width Modulation
PCC	-	Point of Common Coupling
VFC	-	Voltage Frequency Controller
SPS	-	Sim Power System
VF	-	Voltage and Frequency
VSC	-	Voltage Source Converter
ZCD	-	Zero Crossing Detector

---

---

## CHAPTER 1

---

---

## CHAPTER 1

### INTRODUCTION

THERE has been a huge increase in energy demand during the last few decades, which has accelerated the depletion of the world fossil fuel supplies. Environmental concerns and international policies are supporting new interests and developments for small scale off grid power generation. In view of this, self excited asynchronous generators have regained importance for supplying electricity to the remote located communities (where grid supply is not applicable) using available renewable energy sources like wind, hydro and bio-mass. It is well known that for maintaining constant voltage at the terminals of Asynchronous generator under the condition of varying wind speed. In case of constant speed prime mover like biogas, diesel, gasoline engines, the speed of the isolated asynchronous generator remains constant while voltage at the generator terminal varies under varying consumer loads because of increased reactive power requirement. Therefore in such application of IAG, reactive power compensators have been proposed such as SVC, STATCOM etc [1]. Therefore in such constant power prime mover applications of IAG, electronic load controllers have been recommended.

The proposed isolated wind energy system maintain the constant output power at the generator terminal so that the frequency of the output voltage can be maintained constant at rated power while the voltage is maintained constant with fixed excitation. However, in application such as wind power both input power and speed are varying which in turn varies the magnitude and frequency of the generated voltage of the IAG under the condition of varying wind speed. However, substantial literature is available in remote located wind power application employing asynchronous generators. Some of application has been used squirrel cage asynchronous generator, and few have proposed slip ring asynchronous generator for regulating the voltage and frequency by applying electrical or mechanical controls.

Self excited squirrel cage asynchronous generators have several advantages for standalone power applications, such as,

- 1) No need for an external power supply to produce the magnetic field,
- 2) Reduced maintenance,
- 3) Rugged and
- 3) Simple construction due to brushless rotor.

But, major hurdles in the area of their commercialization are poor voltage and frequency regulation with speed or load variations. A number of attempts have been made to investigate the controller for isolated asynchronous generator (IAG) in constant power and constant speed. Therefore in this project, an attempt is made to investigate a solid state controller for regulating the voltage and frequency of an isolated asynchronous generator supplying a three phase load. In this project, an investigation has been made to explore new control algorithm for the VFC of IAG in the wind power generation [2].

The proposed Voltage Frequency Controller is based on  $I\cos\phi$  current detection method for generation of reference source current [6]. The two-leg voltage source converter (VSC) with split capacitor is used along with a BESS as a VFC to feed three phase loads. The VFC is isolated from the point of common coupling (PCC) through the isolated transformer. The use of isolation transformer reduces the VSC switches rating and with the two-leg VSC, the numbers of controllable switch count are reduced [8]. In this system a delta connected excitation capacitor bank is connected across the generator terminals with required value such that generator develops the rated terminal voltage under no-load and rated speed of IAG. In  $I\cos\phi$  algorithm, it is considered that the generator supplies only the real component of load currents, 'I' the amplitude of fundamental real component of the load current and  $\cos\phi$  the displacement angle of fundamental real component of the load current with respect to the source voltage. The reactive power compensation for the load current and regulation of terminal voltage under varying load conditions are taken care by VFC

## 1.2 OBJECTIVES OF THE PROJECT

The main objective of this project to maintain the terminal voltage and frequency of isolated induction generator are constant. This project deals with the  $I \cdot \cos\phi$  algorithm for the voltage and frequency control (VFC) of an autonomous wind power generation using an isolated asynchronous generator (IAG) three phase loads. The reference source currents are estimated using the  $I \cdot \cos\phi$  algorithm to control the voltage and frequency of IAG system. Two-leg voltage source converter (VSC) with split capacitor and an isolation transformer is used as an integrated VSC. The reduced switch integrated VSC with a battery energy storage system (BESS) is used for the power management of the wind energy conversion system (WECS). Bi-directional power flow capabilities of the proposed voltage and frequency (VF) controller in WECS are demonstrated through simulation results. The proposed VF controller functions as a voltage regulator in the WECS.

## **1.4 ORGANIZATION OF THESIS**

This gives an overall outline of the project report.

### **CHAPTER 1**

It describes the general introduction and objective.

### **CHAPTER 2**

It describes the block diagram of standalone wind power system

### **CHAPTER 3**

It describes Control Circuit for the proposed two leg voltage source Converter

### **CHAPTER 4**

It includes the introduction MATLAB (simulink), simulation details of individual block and simulation results of the system.

### **CHAPTER 5**

It includes the proposed system model and description of all components used in the hardware. It shows the schematic diagram of the hardware and output waveforms and test results.

### **CHAPTER 6**

Gives the conclusion.

---

---

## CHAPTER 2

---

---

## Chapter 2 Methodology

### 2.1 EXISTING THREE LEG CONVERTER

The existing controller includes three-phase insulated gate bipolar junction transistor (IGBT) based voltage source converter (VSC) along with a battery at excitation capacitor is selected to generate the rated voltage at its dc link. The controller is connected at the point of common coupling (PCC) through the inter-facing inductor

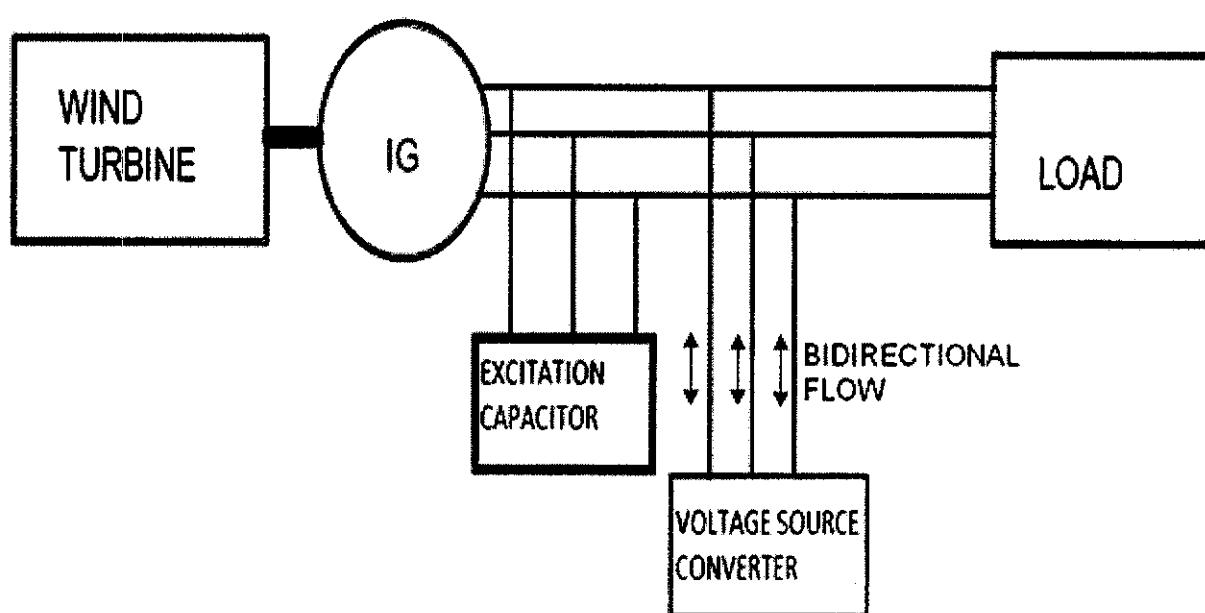


Fig.2.1 Standalone alone induction generator with three leg voltage source converter

The existing controller is having bidirectional flow capability of reactive and active powers because of which it can control the magnitude and frequency of the generated voltage under different electrical and mechanical dynamic conditions. Accordingly the principle of frequency regulation for generating constant frequency at fixed speed, the total generated power should be consumed by the applied load (consumer load battery) otherwise additional generated power might be stored in the revolving component of the machine and it increases the machine speed which in turns increases the system frequency. On the other hand when there is variation in wind speeds and corresponding variation in the machine speed, the battery and consumer

loads absorb such amount of power by which desired frequency of the generated voltage can be achieved. In proposed control scheme, the frequency controller is used for extracting active component of the source current. When there is deficiency in the generated power, the battery supplies the additional required load demand through process of discharging and maintains the constant frequency along with providing the functions of load leveling [21]–[23]. While there is an excess generated power it starts charging and consumes additional generated power which is not consumed by the consumer loads.

Advantage of existing method:

- 1) Induction generator used in this is simple, reliable, cheap, lightweight, and requires very little maintenance.
- 2) Constant output voltage.
- 3) Constant output frequency.
- 4) Reactive power needed for induction generator is taken from capacitor bank itself, not need to taken from grid.

## 2.2 SIMULATION OUTPUT

The simulation output has been taken for the input parameters of 7.5kw,320 voltage,50Hz.The magnitude of three phase output voltage and its frequency has maintained constant for different wind speed as show in the below simulation diagram. In this project the modelling and simulation of the system is done using MATLAB (using simulink and power system block set tool boxes).

### 2.2.1 CONSTANT OUTPUT VOLTAGE

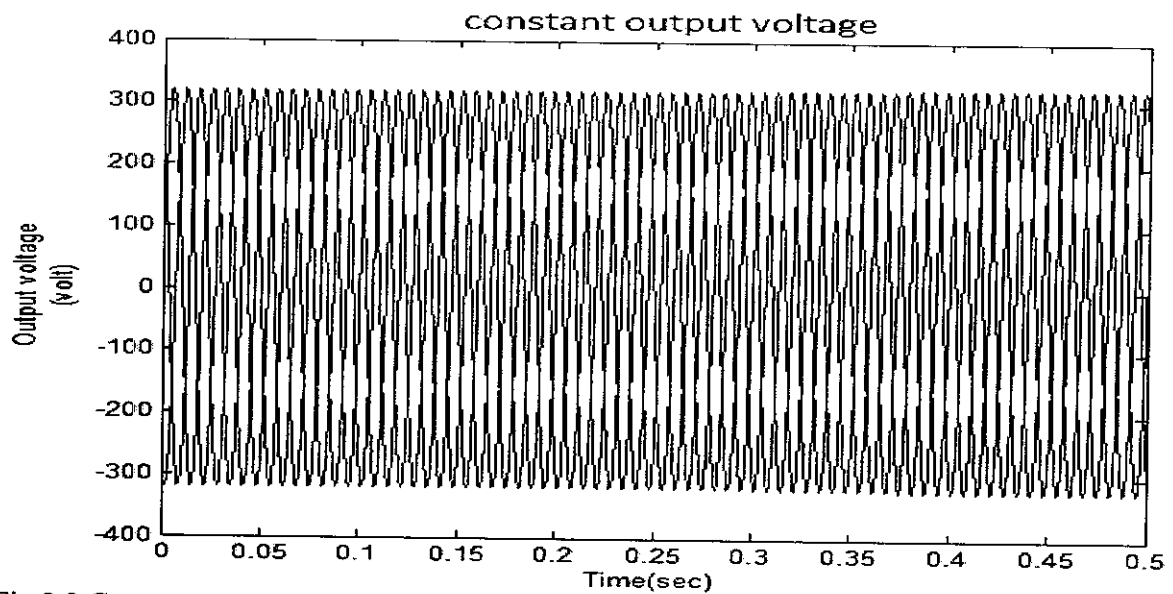


Fig.2.2 Constant output voltage

### 2.2.2 CONSTANT OUTPUT FREQUENCY

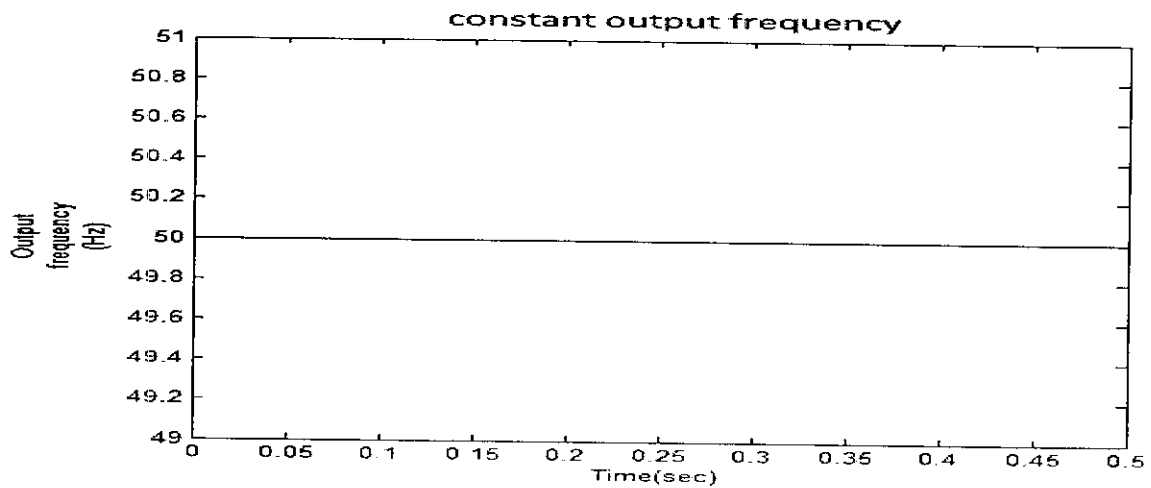


Fig.2.3 Constant output frequency

The diagram shows that the magnitude of input voltage 320 volts input frequency 50Hz has been maintained at the output side constantly for the different wind speeds. It has been observed that the existing controller has been found to regulate the magnitude frequency of the generated voltage constant in isolated wind power application.

### 2.2 PROPOSED TWO LEG CONVERTER

The proposed controller includes two-leg voltage source converter (VSC) with split capacitor is used along with a BESS as a VFC to feed three phase load. The controller is connected at the point of common coupling (PCC) through the inter-facing inductor.

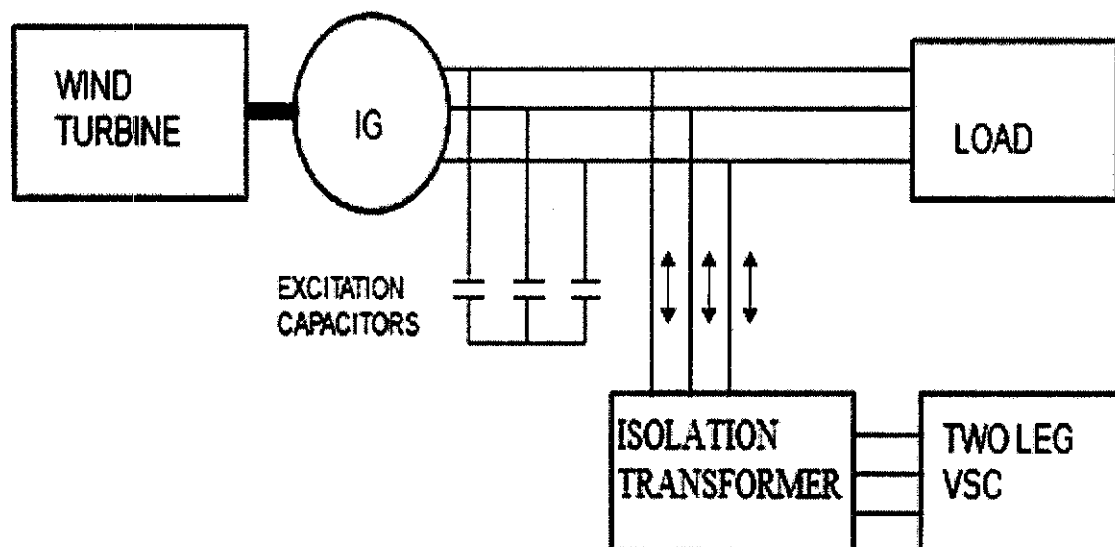


Fig 2.4 block diagram of proposed two leg VFC in standalone wind power system

In this proposed method, a new control algorithm has been used for the VFC of IAG in the wind power generation. The proposed VFC is based on  $I_{cos\phi}$  current detection method for generation of reference source current [6]. The VFC is isolated from the point of common coupling (PCC) through the isolation transformer. The use of isolation transformer reduces the VSC switches rating and with the two-leg VSC, the numbers of controllable switch count are reduced [7]. In this system a delta connected excitation capacitor bank is connected across the generator terminals with required value such that generator develops the rated terminal voltage under no-load and rated speed of IAG.

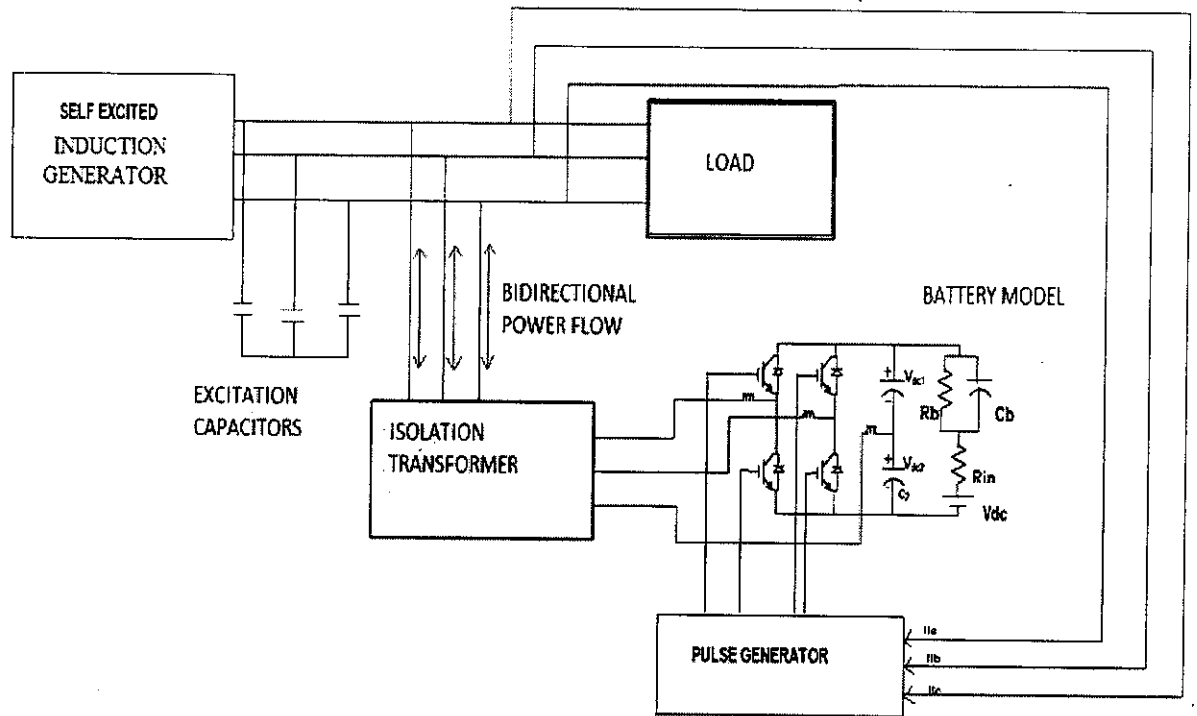


Fig 2.5 circuit diagram of two leg converter in standalone wind power generation

The controller used in this wind power system having bidirectional power flow capability. When at the time of excess power generated from self excited induction generator the battery charges that surplus power which is not consumed by the consumer load and when there is deficiency in the generated power, the battery supplies the additional required load demand through process of discharging and maintains the constant frequency.

Advantage of proposed method:

- 1) Using isolation transformer switch rating can be reduced,
- 2) Reduced switch.(only four IGBT for three phase VSC),
- 3) Constant output voltage,
- 4) Constant output frequency.

---

---

## CHAPTER 3

---

---

Moreover, the quadrature unit templates are computed as,  $U_{ap}, U_{bp}$  and  $U_{cp}$ . The expression for these quadrature unit templates is given by

$$\begin{aligned} u_{aq} &= (-u_{ap} + u_{cp}) / \sqrt{3}. \\ u_{bq} &= (u_{ap} \sqrt{3} + u_{bp} - u_{cp}) / \sqrt{3}. \\ u_{cq} &= (-u_{ap} \sqrt{3} + u_{bp} - u_{cp}) / (2\sqrt{3}); \end{aligned}$$

### 3.1.3 Estimation of source frequency

The frequency of terminal voltages is estimated using inphase and quadrature unit templates. The in-phase unit templates are in phase with source voltages, so it can be considered as a sinusoidal function rotating at an angular frequency of the source voltage. The quadrature unit template of phase A is shifted from in-phase unit template by an angle of 90 degree, so it can be treated as a cosine function rotating with a source angular frequency. Therefore the source frequency  $\omega_{ms}$  in radian/sec can be given as,

$$\omega_{ms} = \cos \theta p(\sin \theta) - \sin \theta p(\cos \theta)$$

where  $p$  is the time derivative operator,  $\sin \theta = U_{ap}$ ,  $\cos \theta = U_{aq}$ , and IAG frequency is as  $f = \omega_{ms}$

### 3.1.4 Estimation of fundamental reference real power

The amplitude  $IL_1 \cos \phi$  is the active power component of the respective fundamental load currents. This is extracted as the amplitude of the fundamental load current, phase shifted by 90 degree, at the negative zero-crossing of the phase voltage. A second order low pass filter with a cut-off frequency of 50 Hz is used to extract the fundamental load current with an inherent phase shift of 90 degree. A ZCD is used to detect the negative zero crossing of the corresponding in-phase unit templates. The phase-shifted amplitude of fundamental real power component of the load current is held as the sample input and ZCD output is considered as the hold input to the SHC. The output of SHC is the  $IL_1 \cos \phi$  amplitude. The amplitude of the three-phase fundamental real power component of the load currents are as follows,

$$I_{Lap} = |I_{La}| \cdot \cos \phi_a \cdot I_{Lsp} = |I_{Lb}| \cdot \cos \phi_b \cdot I_{Lcp} = |I_{Lc}| \cdot \cos \phi_c$$

where  $\phi_a$ ,  $\phi_b$  and  $\phi_c$  are the phase angles of the fundamental currents in a, b and c phases.

### 3.1.5 Extraction of amplitude of fundamental reactive power component of load currents

The amplitude  $IL1.\sin\phi$  is the reactive power component of the respective fundamental load currents. This is extracted as the amplitude of the fundamental load current, phase shifted by 90 degree, at the negative zero-crossing of the quadrature phase voltage. The fundamental load current already extracted is used here. A ZCD is used to detect the negative zero crossing of the corresponding quadrature unit templates. The phase shifted amplitude of fundamental reactive component of the load current is held as the sample input and ZCD output is considered as the hold input to the SHC. The output of SHC is the  $IL1.\sin\phi$  amplitude.

$$I_{Laq} = |I_{La}| \cdot \sin \phi_a, I_{Lbq} = |I_{Lb}| \cdot \sin \phi_b, I_{Lcq} = |I_{Lc}| \cdot \sin \phi_c$$

### 3.1.6 Estimation of fundamental reference real power component of source currents

The average amplitude of the fundamental real power component of the load currents is subtracted from the sum of the output of the frequency PI controller and the output of dc voltage PI controller to estimate the amplitude of the fundamental reference real power component of source currents. The frequency error is given as,

$$f_e(n) = f_{rf}(n) - f(n),$$

where

$f_{rf}$  the reference frequency ( i.e. 50 Hz in this case) and “ $f$ ” is the frequency of the terminal voltage of an IAG. The instantaneous value of “ $f$ ” is estimated as discussed above in equation (5).

At the  $n$ th sampling instant, the output of the frequency PI controller is as,

$$I_{\phi}(n) = I_{\phi}(n-1) + k_{ff} \{f_e(n) - f_e(n-1)\} + k_{fv} f_e(n)$$

Similarly the error between two capacitor voltages is given as,

$$V_{dce}(n) = V_{dc1}(n) - V_{dc2}(n)$$

Where

$V_{dc1}$  is the voltage across upper-side capacitor at the dc bus and  $V_{dc2}$  is the voltage across the lower-side capacitor.

At the  $n$ th sampling instant, the output of the voltage PI controller is as,

$$I_{\hat{d}cp}(n) = I_{\hat{d}cp}(n-1) + k_{pi} \{V_{\hat{d}ce}(n) - V_{\hat{d}ce}(n-1)\} + k_{pf} V_{\hat{d}ce}(n)$$

Therefore the amplitude of fundamental reference real source current is as,

$$I_p = I_f + I_{LP}$$

Where,

$$I_f = I_{fp} + I_{dcp}, \quad I_{LP} = (I_{Lap} + I_{Lbp} + I_{Lcp}) / 3.$$

For the two-leg VSC, only two phase currents need to be controlled, the third-leg control is inherent. Therefore the fundamental reference real power components of the source currents for two phases A and B are given as,

$$\hat{i}_{sap}^* = I_p u_{ap}, \quad \hat{i}_{sbp}^* = I_p u_{bp}.$$

### 3.1.7 Estimation of fundamental reference reactive power component of source currents

The average amplitude of the fundamental reactive power component of the load currents is subtracted from the voltage PI controller output to estimate the amplitude of the fundamental reference reactive power component of the source currents. The ac voltage error at the nth sampling instant is given as,

$$V_e(n) = V_r(n) - V(n)$$

where  $V_r(n)$  is the amplitude of the reference ac terminal phase voltage and  $V(n)$  is the amplitude of the sensed three phase ac voltage at PCC is computed as given in equation .

The output of the voltage PI controller for maintaining a constant ac terminal voltage at the nth sampling instant is expressed as

$$I_{vq}(n) = I_{vq}(n-1) + k_{pi} \{V_e(n) - V_e(n-1)\} + k_{pf} V_e(n)$$

where  $k_{pi}$  and  $k_{pf}$  are the proportional and integral gain constants of the PI controller.  $V_e(n)$  and  $V_e(n-1)$  are the voltage errors in the nth and (n-1)th sampling instant and  $I_{vq}(n)$  and  $I_{vq}(n-1)$  is the output of voltage PI controller in the nth and (n-1)th instant needed for the voltage control.

Therefore the amplitude of fundamental reference reactive power components of the source current is given as,

$$I_q = I_{vq} - I_{Lq}$$

Where

$$I_{Lq} = (I_{Laq} + I_{Lbq} + I_{Lcq}) / 3.$$

Two phase fundamental reference reactive power component of the source currents for phase A and B are given as,

$$i_{saq}^* = I_g M_{aq}, \quad i_{sbq}^* = I_g M_{bq},$$

### 3.1.8 Estimation of fundamental power component of reference source currents

Two-phase fundamental power component of the reference source currents are estimated for each phase as the vector sum of individual phase,

$$i_{sa}^* = i_{sgsp} + i_{saq}, \quad i_{sb}^* = i_{sbsp} + i_{sbq},$$

### 3.1.9 PWM Generator

These reference source currents ( $i_{sa}^*$ ,  $i_{sb}^*$ ) are compared with sensed source currents ( $i_{sa}$ ,  $i_{sb}$ ). The resulting current errors are amplified using the proportional controller by gain “K” and Amplified signals are compared with fixed-frequency (10 kHz) triangular carrier wave to generate the gating signals for the VSC switches of VFC [5].

## 3.2 MODELING OF THE MECHANICAL SYSTEM:

The mechanical power generated by a wind turbine in per unit system is given as,

$$P_{mpu} = 0.5 \rho A c_{ppu} v_{windpu}^3$$

where  $P_m$  per unit is the power in per unit of nominal power for particular value of specific density of air ( $\rho$ ) and the swept area of blades ( $A$ ).  $C_p$  per unit is performance coefficient in per unit of maximum value of power coefficient,  $v$  wind per unit is the wind speed in per unit of the base wind speed. The base wind speed is the mean value of expected wind speed in m/s.

To generate a constant frequency, ideally the additional generated power with the increased wind speed is stored into the battery and the speed of the IAG is maintained constant.

A generic equation is used to model  $c(\lambda, \beta)$ . The equation based on the modeling turbine characteristics is as,

$$c_p(\lambda, \beta) = c_1 \left( \frac{c_2}{\lambda_1} - c_3 - c_4 \right) e^{\frac{c_5}{\lambda_1}} + c_6 \lambda$$

$$\frac{1}{\lambda} = \frac{1}{\lambda + 0.008\beta} - \frac{0.038}{\beta^3 + 1}$$

In the present model  $\beta=0$ .

An available model of the wind turbine in per unit system is used to realize the wind power of WECS.

### 3.3 MODELING OF THE VFC

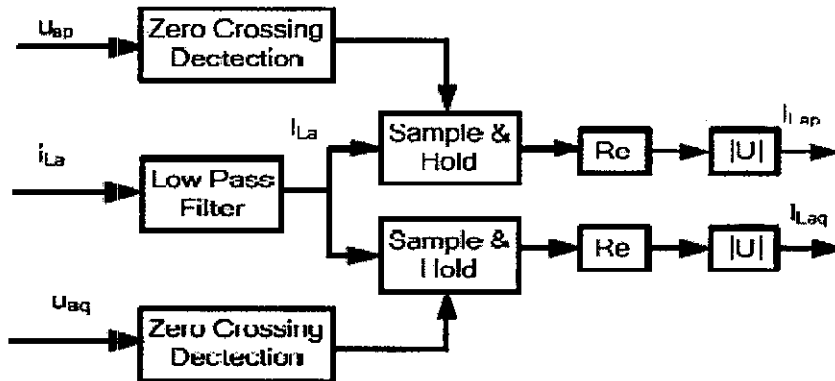


Fig 3.2 Control algorithm block diagram

The proposed  $I_{c}\cos\phi$  based VFC consists of a two leg current controlled voltage source converter (CC-VSC) with split-capacitor as a third leg and the battery at its dc link. The mid-point of three legs are connected individually to each phase of the secondary windings of T-connected transformer shown in Fig. 3. The VSC is isolated from the generator bus through a isolation connected transformer at point of common coupling.

The dc voltage across one capacitor is given as follows,

$$V_{c1} \geq (2\sqrt{2})V / m$$

where  $m$  is the modulation index and  $V$  is the rms value of phase voltage.

Therefore the battery voltage must be given as follows,

$$V_b \geq 2(2\sqrt{2})V / m$$

Since the battery is an energy storage unit, its energy is represented in kilowatt-hours (kWh),

When a capacitor is used to model the battery unit, its capacitance  $C_b$  can be determined as follows,

$$C_b = \frac{kWh * 3600 * 10^3}{0.5(v_{oc\ max}^2 - v_{oc\ min}^2)}$$

where

$V_{oc\ max}$  and  $v_{oc\ min}$  are the maximum and minimum open circuit voltage of the battery under fully charged and fully discharged conditions. In the equivalent model,  $R_{in}$  is the equivalent series resistance of the parallel /series combination of a battery, which is usually a small value. The parallel circuit of  $C_b$  and  $R_b$  is used to describe the stored energy and the resistance responsible for self discharging.

---

---

## CHAPTER 4

---

---

## CHAPTER 4

### 4.1 MATLAB

The name MATLAB stands for matrix laboratory. MATLAB is a high-performance language for technical computing. It integrates computation, visualization, and programming in an easy-to-use environment where problems and solutions are expressed in familiar mathematical notation. In this project the modeling and simulation of the proposed system is done using MATLAB (using simulink and power system block set tool boxes).

### SIMULINK

Simulink is a software package for modeling, simulating, and analyzing non linear dynamical systems. It is a graphical mouse-driven program that allows somebody to model a system by drawing a block diagram on the screen and manipulating it dynamically. Simulink is a platform for multi domain simulation and Model-Based Design for dynamic systems. It provides an interactive graphical environment and a customizable set of block libraries, and can be extended for specialized applications.

### POWER SYSTEM BLOCK SET

The Power System Block set allows scientists and engineers to build models that simulate power systems. The block set uses the Simulink environment, allowing a model to be built using click and drag procedures. Not only can the circuit topology be drawn rapidly, but also the analysis of the circuit can include its interactions with mechanical, thermal, control, and other disciplines. Sim Power Systems extends Simulink with tools for modelling and simulating basic electrical circuits and detailed electrical power systems. These tools let you model the generation, transmission, distribution, and consumption of electrical power, as well as its conversion into mechanical power. Sim Power Systems is well suited to the development of complex, self-contained power systems, such as those in automobiles, aircraft, manufacturing plants, and power utility applications



The circuit configuration of the proposed two leg converter is applied to the three-phase three-wire induction generator system. The three-phase three-wire induction generator is driven by a wind turbine and generates power for the utility, and the reactive power is supplied from the delta connected excitation capacitors. The proposed converter consists of two leg VSC and battery. The isolation transformer used in this system is to reduce switch rating.

The two leg voltage source converter is to control the voltage and frequency from the generator output. The battery used to store the surplus power and its discharge while at any deficiency in power generation. The utility of the stand alone wind power system is RL load.

#### 4.2.3 CONTROL CIRCUIT OF PROPOSED POWER CONVERTER

The operation of VFC enforces to maintain the rated terminal voltage under varying load conditions and to maintain a constant supply frequency along. To achieve this, the reference source currents need to be controlled through proper switching of VSC switches. The reference source currents have two parts for each phase, one is real power component i.e.  $I \cos\phi$  and other is reactive power component i.e.  $I \sin\phi$ . Both of these components are estimated for each phase. The line voltages  $v_{ab}$  and  $v_{bc}$  are sensed to compute the three phase voltages. A set of in-phase and quadrature unit templates are computed using the fundamental phase voltages. Three phase load currents are sensed and filtered using a 2nd order low pass filter with inherent phase shift of 90 degree to extract the amplitude of the fundamental component of three-phase load currents .

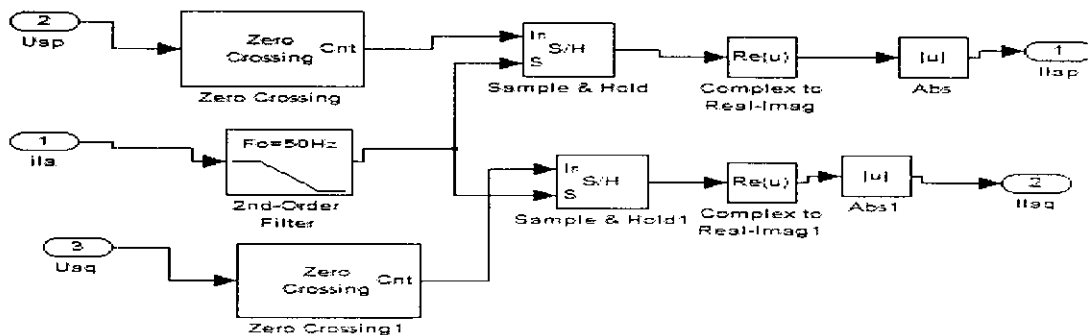


Fig 4.2.  $I \cos\Phi$  algorithm simulation diagram

A zero crossing detector (ZCD) is used to detect the negative going zero-crossing of the corresponding phase voltage. The phase-shifted fundamental current is held as the sample input and ZCD output pulse is as a hold input to the sample and hold circuit (SHC) which output is 'ILp' as an amplitude. The output of the frequency PI controller is treated as 'Ifp' and the output of dc voltage proportional-integral (PI) controller as 'Idcp'. The average of three-phase real power component of the load currents is derived using summing amplifier with a gain (1/3) for load balancing. The algebraic difference between the sum (ILp and Idcp) and average of three-phase load currents (ILap, ILbp, ILcp) estimates the amplitude of real power component of the source currents. Similarly the average of three-phase reactive power component of the load currents is derived from summing amplifier with a gain (1/3) for load balancing. The algebraic difference between the output of the voltage PI controller 'Ivq' and average of three-phase reactive power component of the load currents (ILaq, ILbq, ILcq) computes the amplitude of the reactive power component of the reference source currents

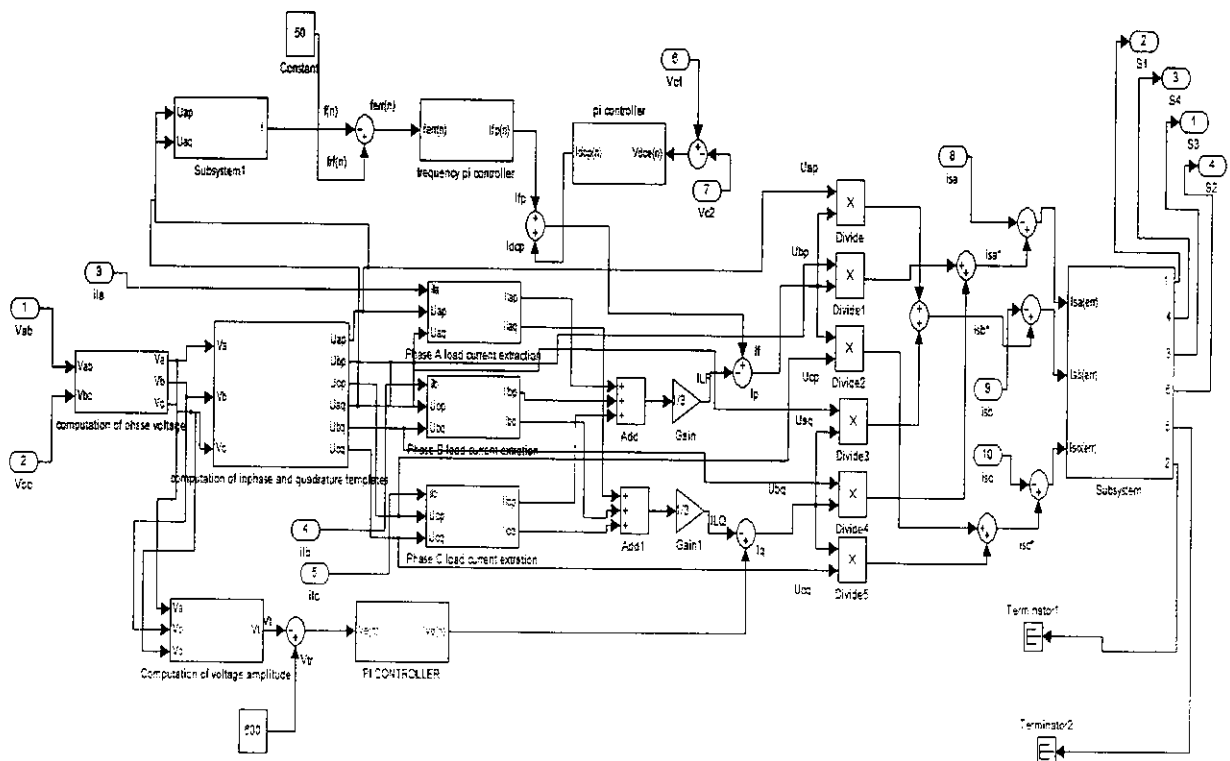


Fig 4.3. Control Circuit of Proposed Power Converter

### 4.3 SIMULATION RESULTS

The proposed  $I \cdot \cos\phi$  based control algorithm of VFC and fixed pitch wind turbine driven IAG is tested with three phase RL load. In order to verify the performance of the proposed two leg converter for standalone wind power generation, a three-phase prototype with a utility line voltage of 700V and a utility frequency of 50 Hz is developed. The simulation output waveforms shows performance of voltage frequency controller with constant output voltage, current and frequency for variable wind speed. This output waveform has taken for the variable wind speed are 8,9,10(m/s) and its instants given at 0,0.1,0.2,0.28(sec)

### 4.4 PARAMETERS:

IAG Data: 275kW, 480V, 50Hz, Y-Connected, 4-pole,  $R_s=0.016\Omega$ ,  $R_r=0.015\Omega$ ,  $L_{ls}=0.006H$ ,  $L_{lr}=0.06H$ ,  $L_m=3.5 H$ .

Wind Turbine Data: 275 kW,  $C_{pmax}=0.48$ ,  $\lambda_m =8.1$ ,  $C_1 =0.5176$ ,  $C_2=116$ ,  $C_3=0.4$ ,  $C_4=5$ ,  $C_5=21$ ,  $C_6=0.0068$ ,  $C_7=0.008$ ,  $C_8=0.035$ .

VFC Data:  $L_f=1mH$ ,  $R_f= 0.05\Omega$ ,  $C_{dc1}=C_{dc2}=7500 \mu F$ ,  $K_{pa}=0.18$ ,  $K_{ia}=20$ ,  $K_{pf}=5$ ,  $K_{if}=250$ ,  $K_{adc}=1$ ,  $K_{idc}=0.1$ .

Battery data:  $C_b=7600 F$ ,  $R_b=10 k\Omega$ ,  $R_{in}=0.1 \Omega$ ,  $nV_{oc} =700 V$ .

### 4.5.OUTPUT VOLTAGE:

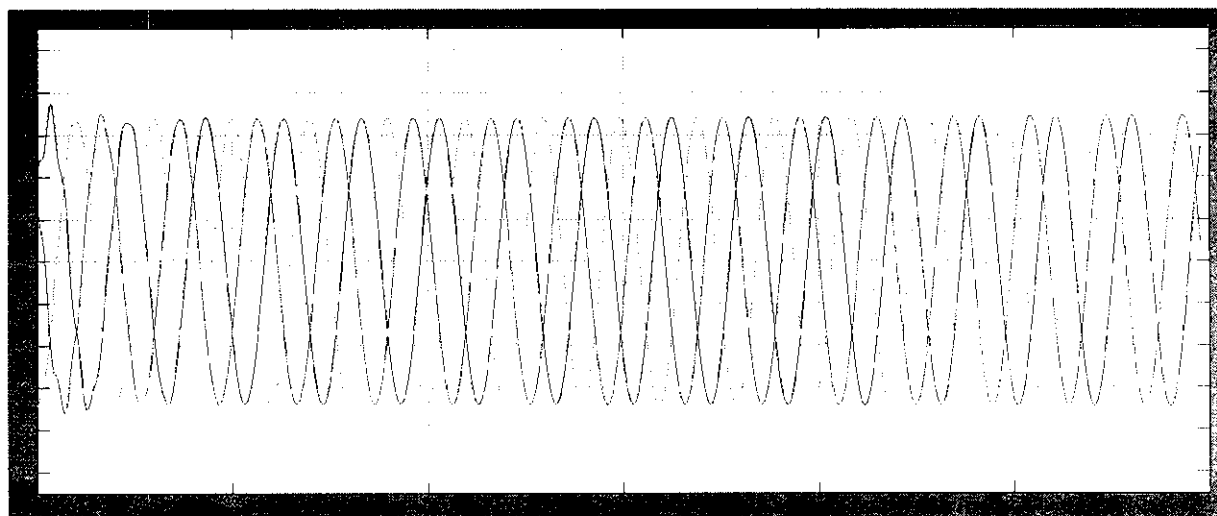


Fig 4.4.constant output voltage of proposed system

#### 4.6.OUTPUT FREQUENCY

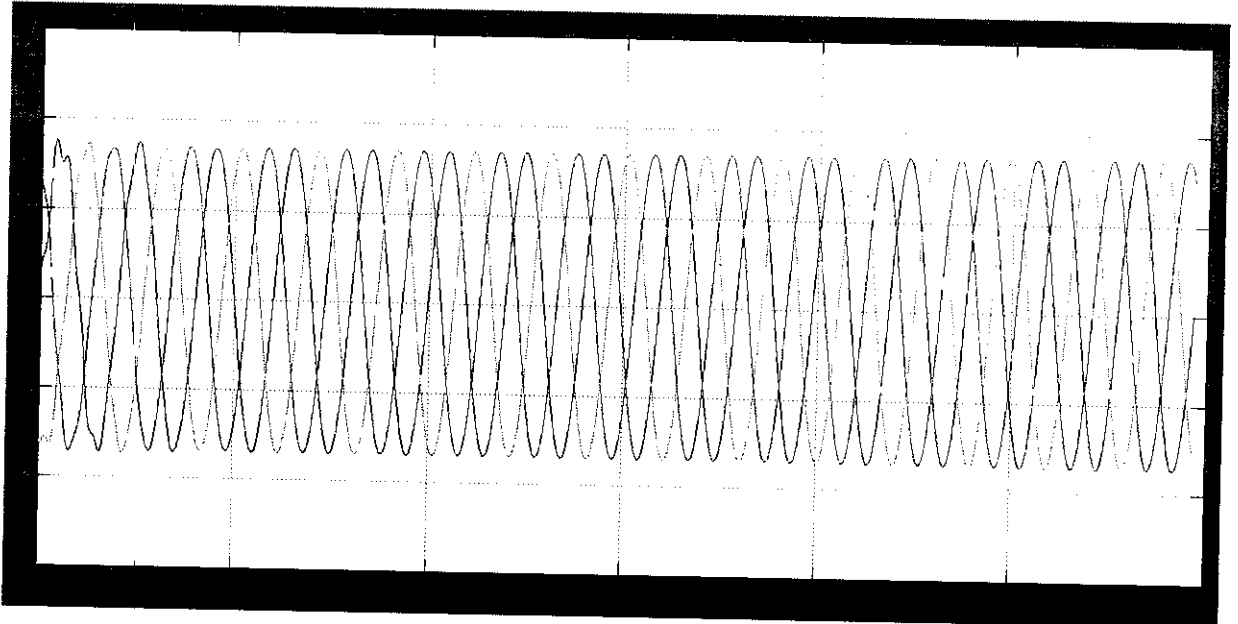


Fig 4.5.constant frequency of proposed system

#### 4.7 OUTPUT CURRENT:

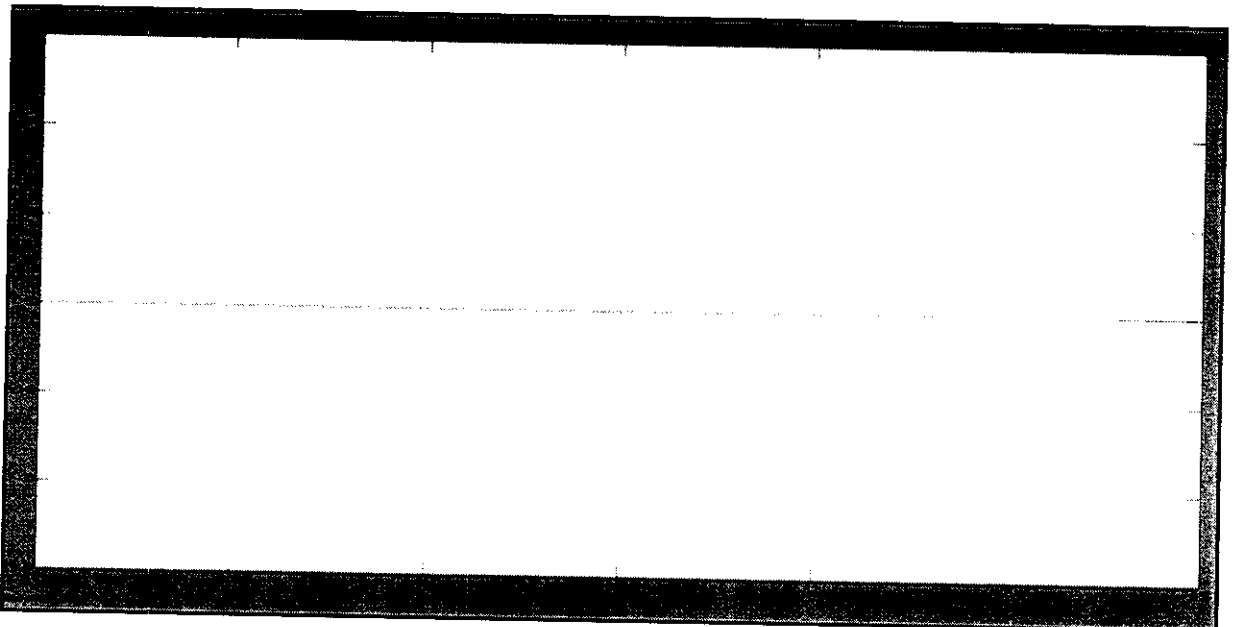


Fig 4.6.Constant output current of proposed system

---

---

## CHAPTER 5

---

---

## CHAPTER 5

### HARDWARE IMPLEMENTATION

#### 5.1 HARDWARE BLOCK DIAGRAM

This chapter explains the block diagram and components used for the hardware prototype of the proposed system. It includes the photographs of the fabricated model and output waveforms. The prototype is done for three phase. The voltage at the secondary side of transformer is reduced to 24V. The schematic is done in AutoCAD.

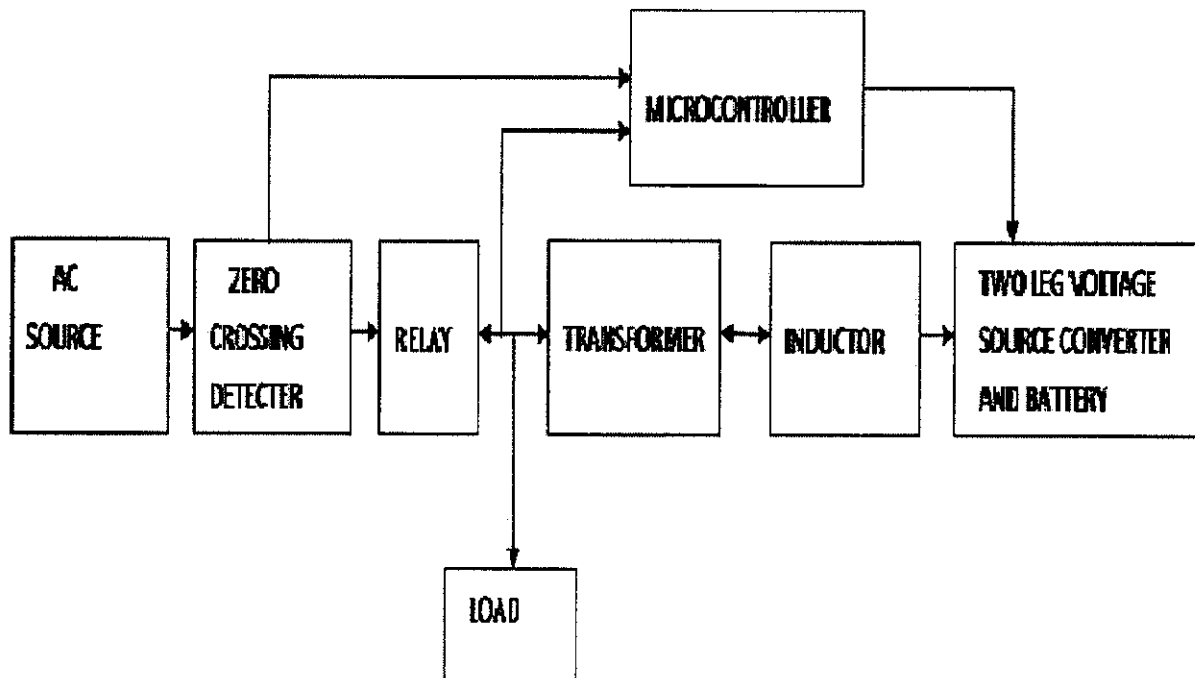


Fig 5.1. Block Diagram of Prototype

The prototype of the proposed system has three phase load, three phase converter and micro controller (PIC16F877A) with 5V power supply. These parts are explained with schematic diagram in following sections. The battery used in this has the rating of 24V. The control signal for the proposed power converter is generated by using the PIC Microcontroller (PIC16F877A).

## 5.2 TWO LEG VOLTAGE SOURCE CONVERTER CIRCUIT WITH LOAD

The three phase proposed power converter circuit with the load is shown in the Fig 5.2. The load is directly fed from the source and the isolation transformer is to isolate the load and power converter. The zero crossing detector is to detect the phase angle of the phase voltage. The optocoupler is to isolate the controller circuit and the power circuit.

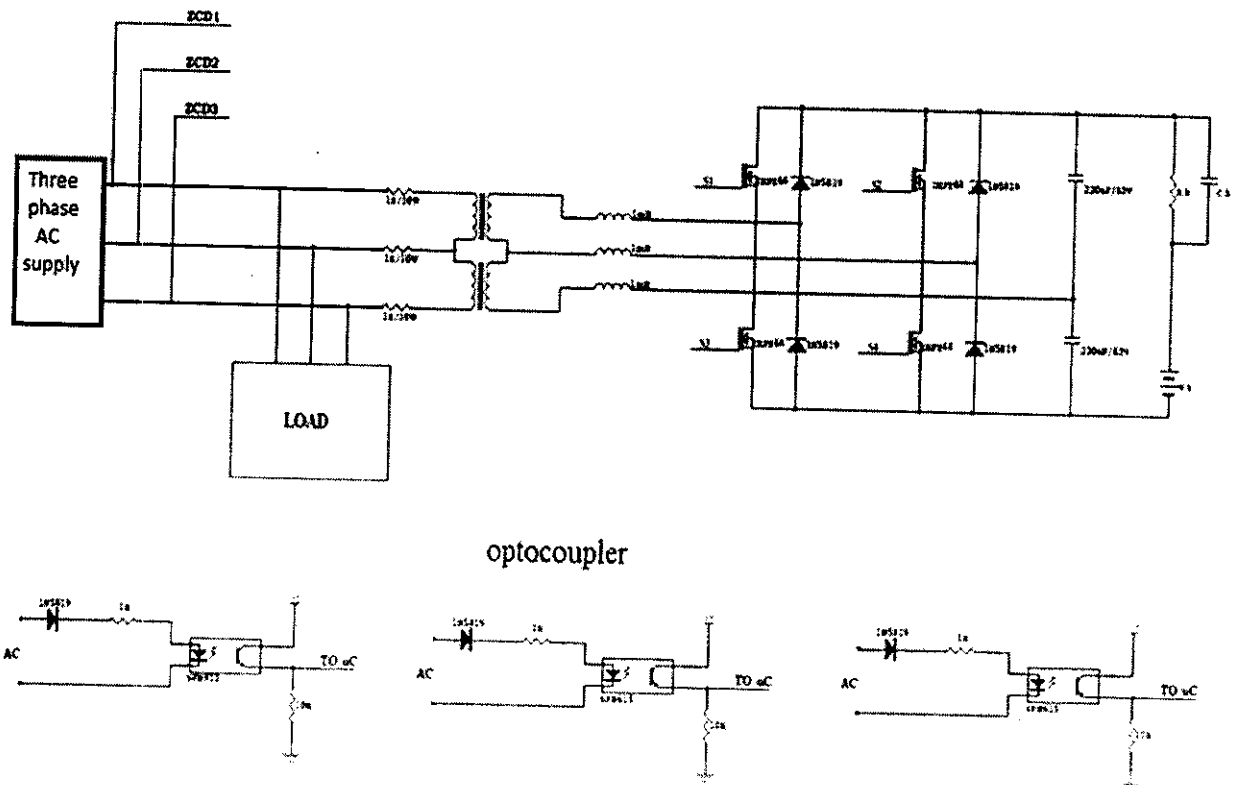


Fig 5.2. Two leg VSC with load circuit

### 5.3 MICROCONTROLLER

The gate pulse for the converter switches are generated by PIC16F877A controller. This micro controller circuit works in 5V power supply. The detail about PIC16F877A is given in APPENDIX I. This controller is isolated from the main circuits by means of opto-coupler. The schematic of micro controller circuit is shown in fig.5.3.

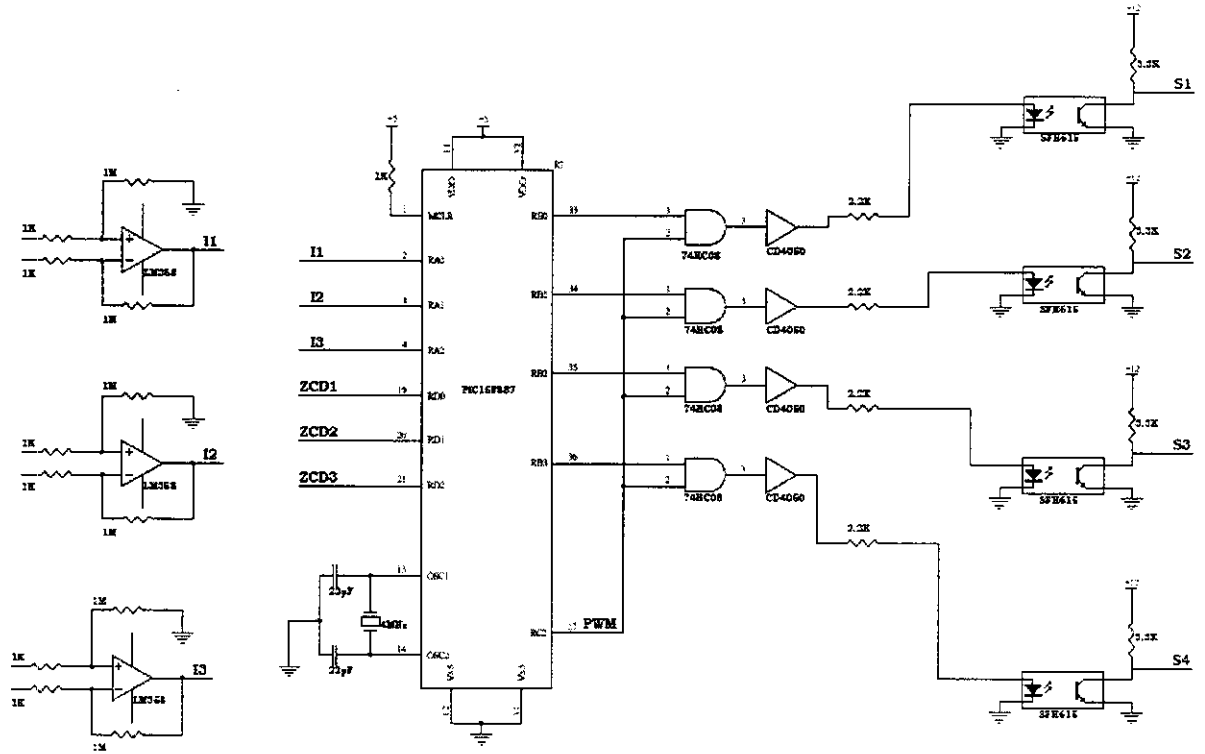


Fig 5.3. Schematic of Microcontroller circuit

The PIC Microcontroller (PIC16F877A) is used to generate the control pulse for the proposed power converter circuit. The output of the PIC controller is connected to the converter circuit through the optocoupler. In this four switching pulses are produced from the microcontroller the operating frequency of the PIC microcontroller is 4MHz.

## 5.4 POWER SUPPLY FOR THE MICROCONTROLLER

Since all electronic circuits work only with low D.C. voltage we need a power supply unit to provide the appropriate voltage supply. This unit consists of transformer, rectifier, filter and regulator. A.C. voltage typically 230V rms is connected to a transformer which steps that AC voltage down to the level to the desired AC voltage.

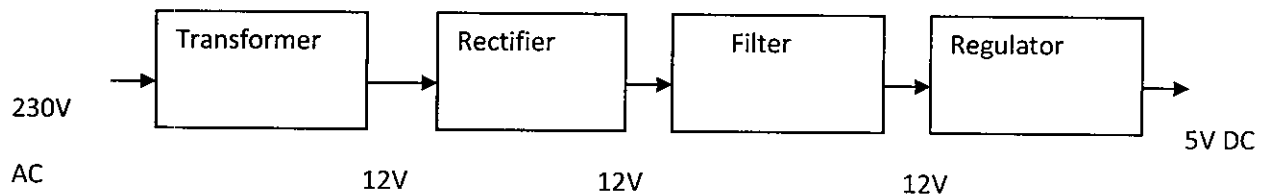


Fig 5.4. Power Supply Block Diagram

A diode rectifier then provides a full-wave rectified voltage that is initially filtered by a simple capacitor filter to produce a DC voltage. This resulting DC voltage usually has some ripple or AC voltage variations. regulator circuit can use this DC input to provide DC voltage that not only has much less ripple voltage but also remains the same DC value even the DC voltage varies somewhat, or the load connected to the output DC voltage changes. The power supply unit is a source of constant DC supply voltage. The required DC supply is obtained from the available AC supply after rectification, filtration and regulation.

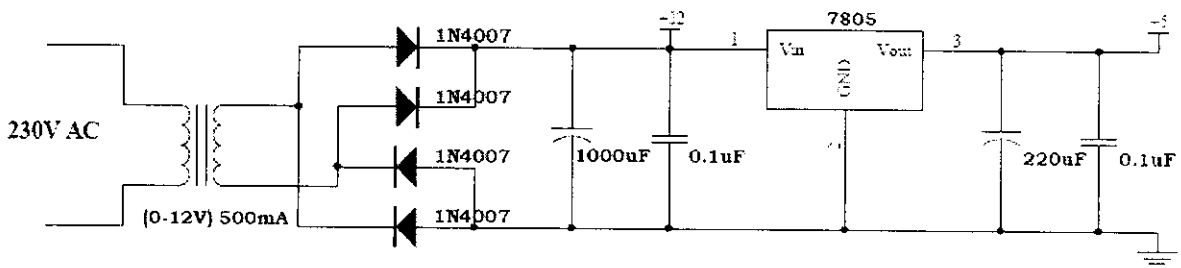
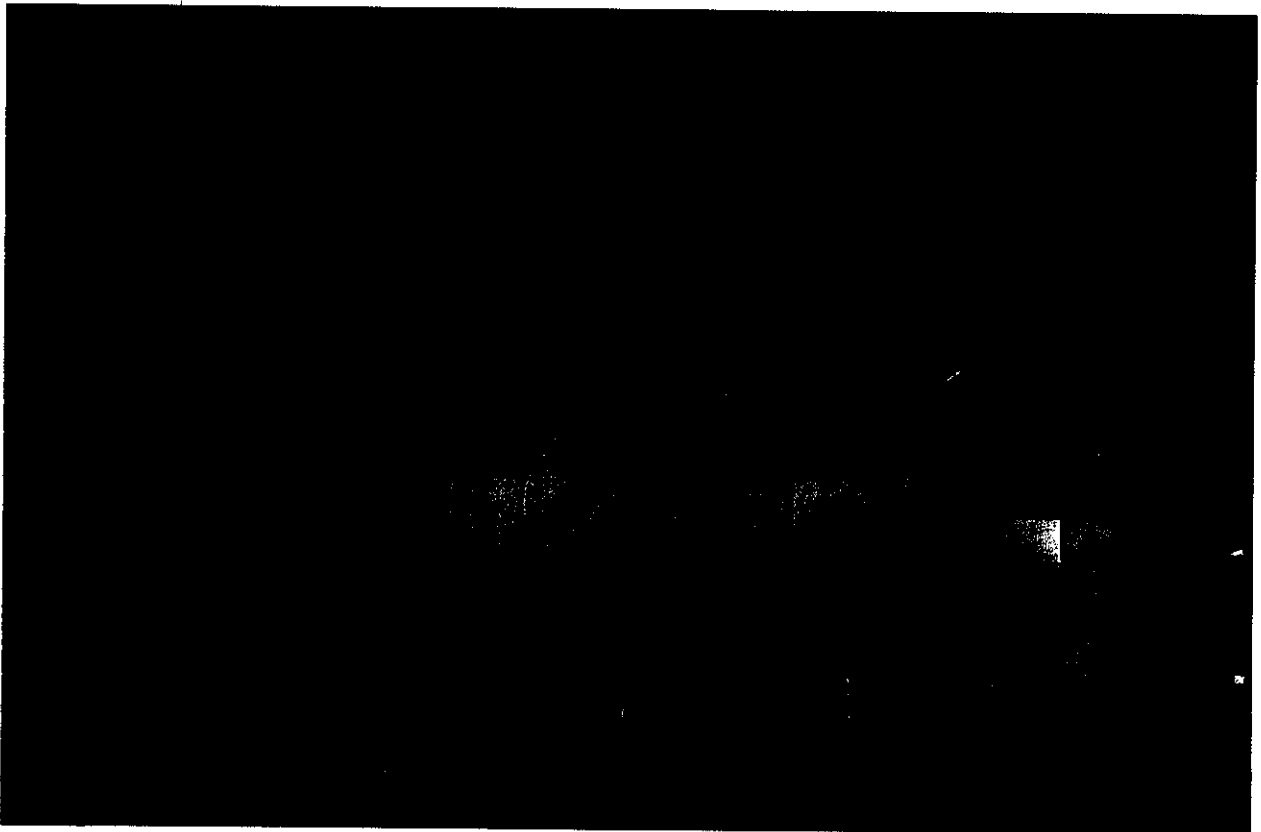


Fig 5.5. Power supply for Microcontroller

## 5.6 PHOTOCOPY OF HARDWARE

The fabricated hardware is shown in below figure 5.1. The output voltage and PWM pattern waveform of the proposed system is shown in figure 5.2 and 5.3. The parts of proposed system are,

- 1) Two leg converter,
- 2) Battery,
- 3) Supply unit,
- 4) Controller.



**Fig 5.1 Hardware photograph.**

## 5.5 HARDWARE TESTING AND RESULTS

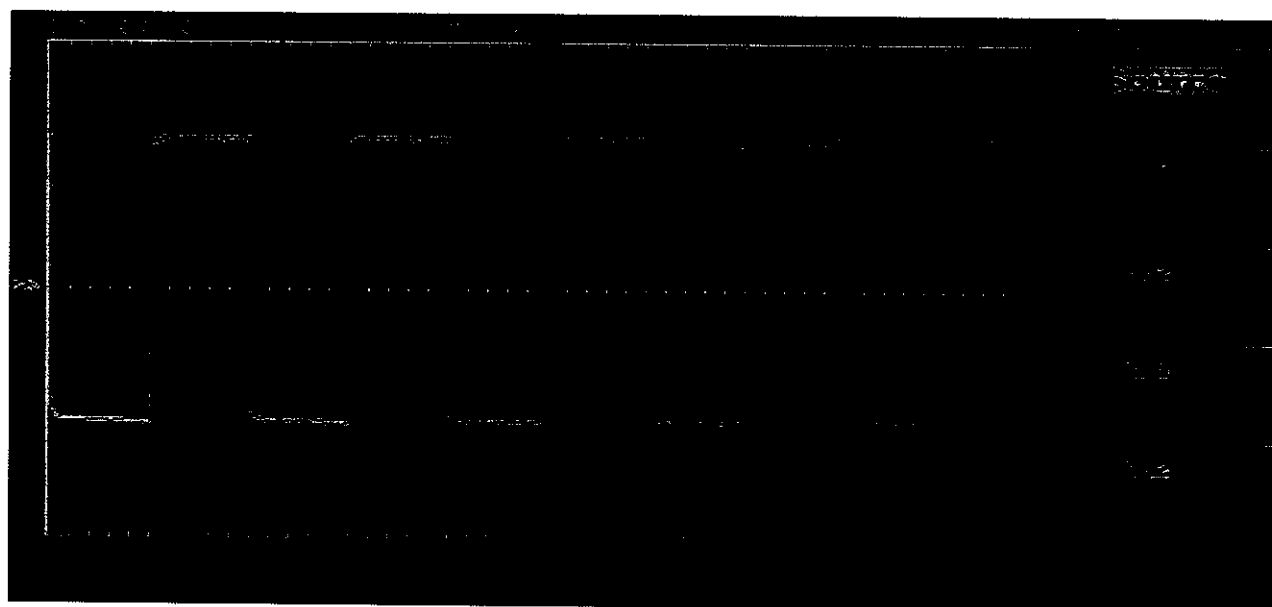


**Fig.5.1 Output voltage waveform**

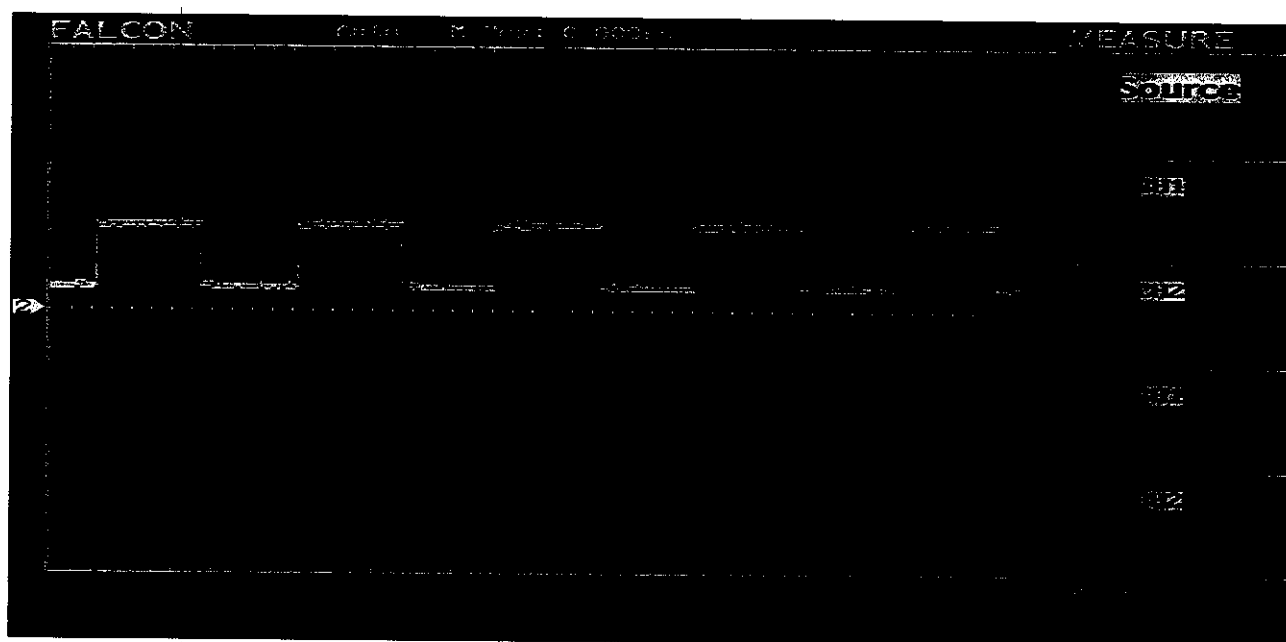


**Fig.5.2 PWM signal for two leg converter**

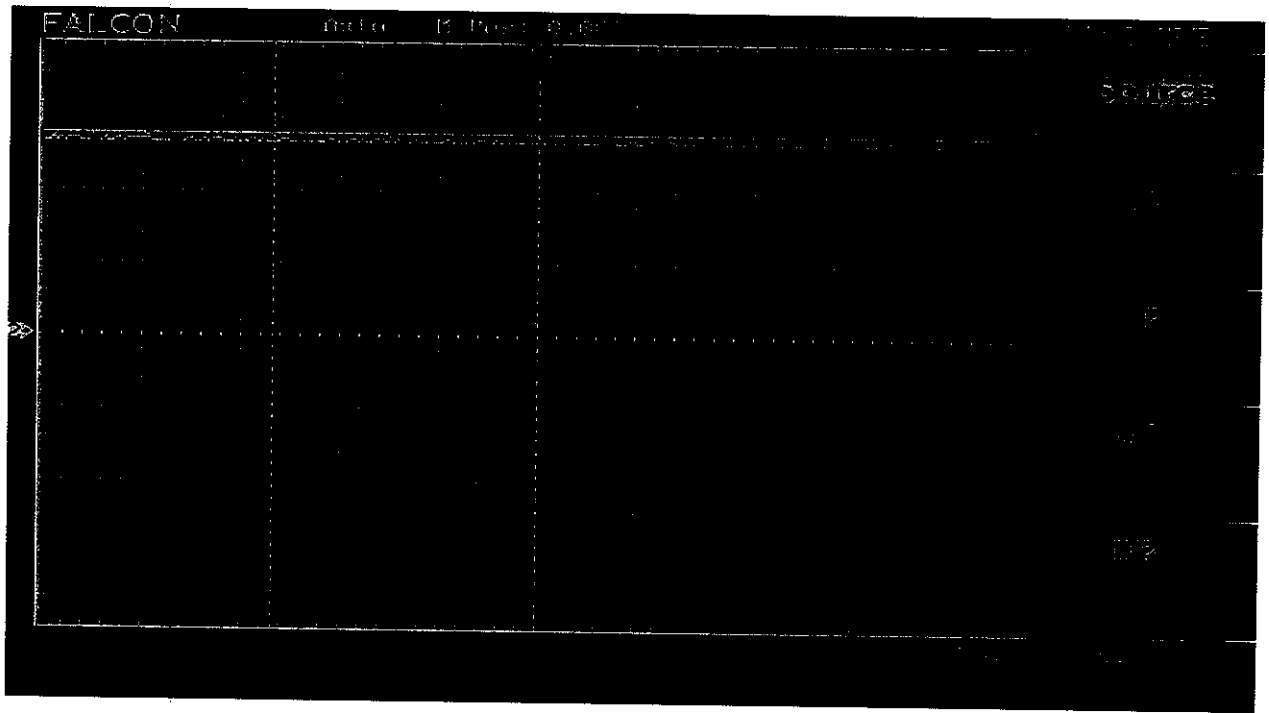


Fig 5.3 battery charging waveform

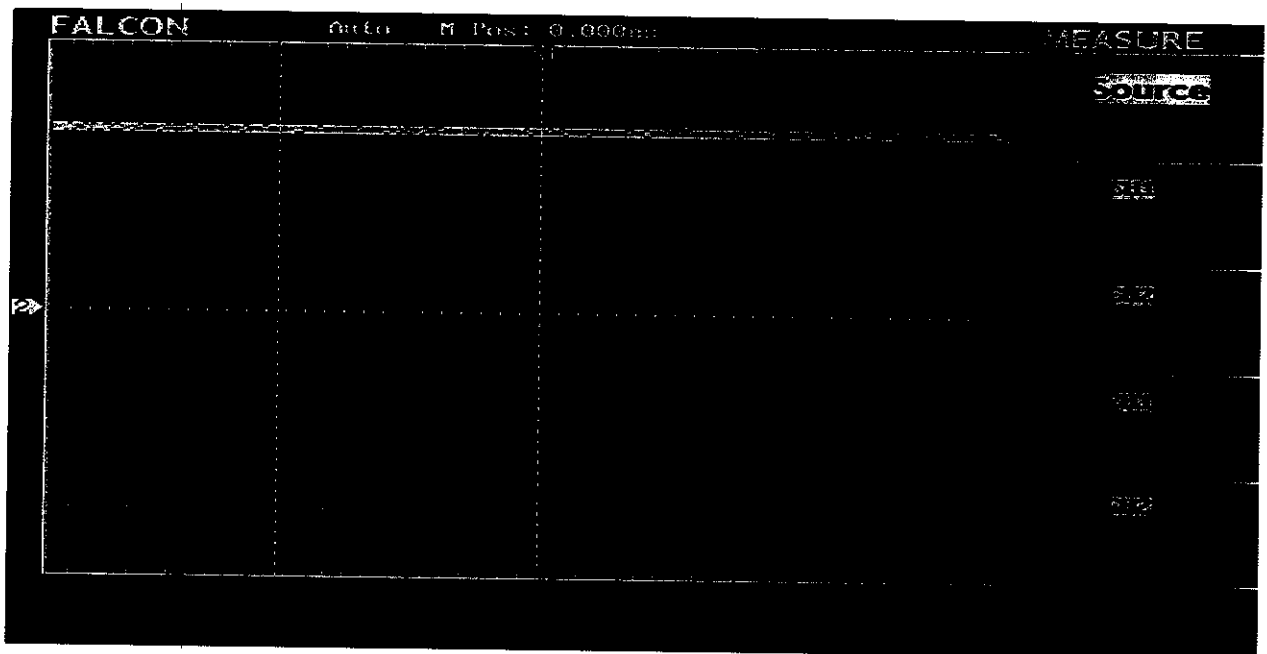


Fig 5.4 battery discharging waveform

---

---

## CHAPTER 6

---

---

## CHAPTER 6

### CONCLUSION

#### 6.1 CONCLUSION

A new control algorithm for voltage and frequency control of IAG has been investigated in isolated WECS. It has been shown that a reduced switch two-leg integrated VSC with a battery energy storage system can be potential candidate as a VFC in isolated direct connected loads. The reduced switch VSC reduces the computational burden of VFC and improves the reliability due to less number of switches. The  $I \cdot \cos\phi$  based algorithm has been verified for the control of VFC in WECS. The simulation results have demonstrated the capabilities of VFC for power quality improvement.

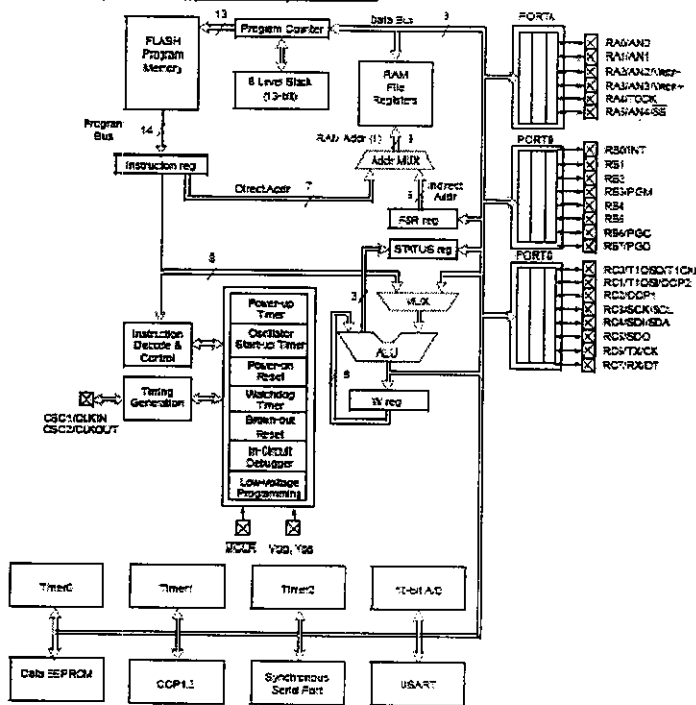
## REFERENCES

- [1] L.L. Lai and T.F. Chan, “*Distributed Generation -Induction and Permanent Magnet Generators*” John Wiley and Sons Ltd, 2007.
- [2] G.K. Kasal and B. Singh, “*Decoupled Voltage and Frequency Controller for Isolated Asynchronous Generators Feeding Three-Phase Four-Wire Loads,*” *IEEE Trans. Power Delivery*, pp. 966 – 973, no.2, vol. 23, April 2008.
- [3] R.M. Hillowala and A.M. Sharaf, “*A rule based fuzzy logic controller for a PWM inverter in a stand -alone wind energy conversion scheme,*” *IEEE Trans. Ind. Appl.*, vol. 32, no. 1, pp. 57-65, Jan./Feb. 1996.
- [4] G.K. Kasal, B. Singh, A. Chandra and K. Al-Haddad, “*Voltage and frequency control with neutral current compensation in an isolated wind energy conversion system,*” in *Proc. IECON 2008*, pp. 2259 – 2264.
- [5] C.V. Nayar and J.H. Bundell, “*Output power controller for wind driven induction generator,*” *IEEE Trans. Aeros. and Electron. Syst.*, vol. 23, no. 3, pp. 388-401, May 1987.
- [6] G. Bhuvaneswari and M.G. Nair, “*Design, Simulation, and Analog Circuit Implementation of a Three-Phase Shunt Active Filter Using the Icos $\phi$  Algorithm,*” *IEEE Trans. Power Delivery*, vol. 23, no. 2, pp. 1222– 1235, April 2008.
- [7] Bhim Singh, P. Jayaprakash and D. P. Kothari, “*A T-Connected Transformer and Three-leg VSC Based DSTATCOM for Power Quality Improvement,*” *IEEE Trans. Power Electron.*, vol. 23, no.6, Nov. 2008.
- [8] H. Akagi, E.H. Watanabe and M. Aredes, “*Instantaneous Power Theory and Applications to Power Conditioning,*” Wiley-Inter-science, IEEE Press, 2007.

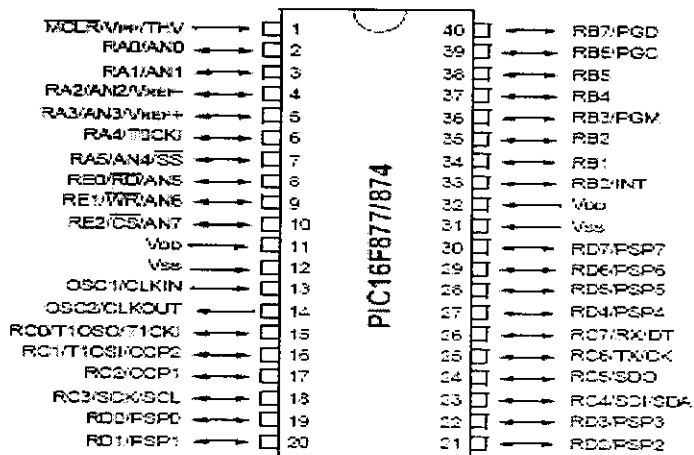
## APPENDIX I

### ARCHITECTURE OF PIC16F877A

Device	Program FLASH	Data Memory	Data EEPROM
PIC16F872	4K	192 Bytes	128 Bytes
PIC16F876	8K	384 Bytes	256 Bytes



### Pin Configuration of PIC16F877A



### TIMER 0 CONTROL REGISTER:

R/W-1	R/W-1	R/W-1	R/W-1	R/W-1	R/W-1	R/W-1	R/W-1
<b>RBPU</b>	<b>INTEDG</b>	<b>T0CS</b>	<b>T0SE</b>	<b>PSA</b>	<b>PS2</b>	<b>PS1</b>	<b>PS0</b>
bit 7							bit 0

bit 7: **RBPU**

bit 6: **INTEDG**

bit 5: **T0CS**: TMR0 Clock Source Select bit

1 = Transition on T0CKI pin

0 = Internal instruction cycle clock (CLKOUT)

bit 4: **T0SE**: TMR0 Source Edge Select bit

1 = Increment on high-to-low transition on T0CKI pin

0 = Increment on low-to-high transition on T0CKI pin

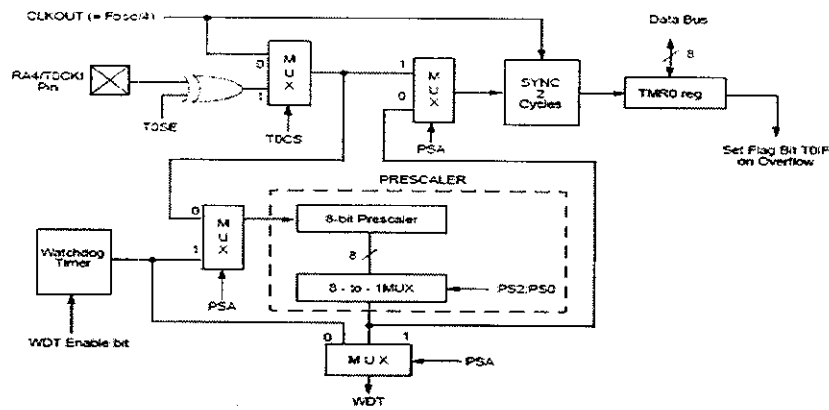
bit 3: **PSA**: Prescaler Assignment bit

1 = Prescaler is assigned to the WDT

0 = Prescaler is assigned to the Timer0 module

bit 2-0: **PS2 PS1 PS0**: Prescaler Rate Select bits

### TIMER 0 BLOCK DIAGRAM:



### TIMER 1 CONTROL REGISTER:

U-0	U-0	R/W-0	R/W-0	R/W-0	R/W-0	R/W-0	R/W-0
—	—	T1CKPS1	T1CKPS0	T1OSCEN	T1SYNC	TMR1CS	TMR1ON
bit7							bit0

bit 7-6: **Unimplemented:** Read as '0'

bit 5-4: **T1CKPS1:T1CKPS0:** Timer1 Input Clock Prescale Select bits

11 = 1:8 Prescale value

10 = 1:4 Prescale value

01 = 1:2 Prescale value

00 = 1:1 Prescale value

bit 3: **T1OSCEN:** Timer1 Oscillator Enable Control bit

1 = Oscillator is enabled

0 = Oscillator is shut off (The oscillator inverter is turned off to eliminate power drain)

bit 2: **T1SYNC:** Timer1 External Clock Input Synchronization Control bit

TMR1CS = 1

1 = Do not synchronize external clock input

0 = Synchronize external clock input

TMR1CS = 0

This bit is ignored. Timer1 uses the internal clock when TMR1CS = 0.

bit 1: **TMR1CS**: Timer1 Clock Source Select bit

1 = External clock from pin RC0/T1OSO/T1CKI (on the rising edge)

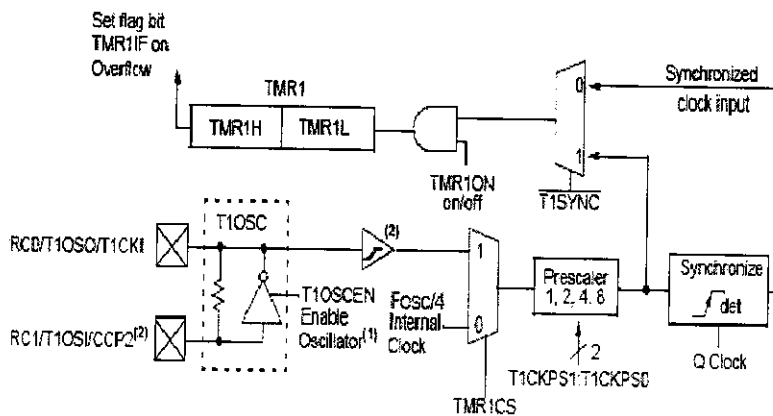
0 = Internal clock (FOSC/4)

bit 0: **TMR1ON**: Timer1 On bit

1 = Enables Timer1

0 = Stops Timer1

### TIMER 1 BLOCK DIAGRAM:



### TIMER 2 CONTROL REGISTER:

U-0	R/W-0	R/W-0	R/W-0	R/W-0	R/W-0	R/W-0	R/W-0
—	TOUTPS3	TOUTPS2	TOUTPS1	TOUTPS0	TMR2ON	T2CKPS1	T2CKPS0
bit7							bit0

bit 7: **Unimplemented**: Read as '0'

bit 6-3: **TOUTPS3:TOUTPS0**: Timer2 Output Postscale Select bits

0000 = 1:1 Postscale

0001 = 1:2 Postscale

0010 = 1:3 Postscale

1111 = 1:16 Postscale

bit 2: **TMR2ON**: Timer2 On bit

1 = Timer2 is on

0 = Timer2 is off

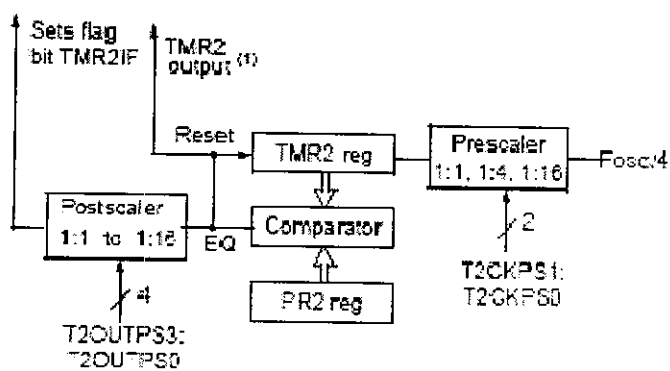
bit 1-0: **T2CKPS1:T2CKPS0**: Timer2 Clock Prescale Select bits

00 = Prescaler is 1

01 = Prescaler is 4

1x = Prescaler is 16

### TIMER2 BLOCK DIAGRAM:



### CCP1CON REGISTER/CCP2CON REGISTER:

U-0	U-0	R/W-0	R/W-0	R/W-0	R/W-0	R/W-0	R/W-0
—	—	CCPxX	CCPxY	CCPxM3	CCPxM2	CCPxM1	CCPxM0
bit7							bit0

bit 7-6: **Unimplemented:** Read as '0'

bit 5-4: **CCPxX :CCPxY:** PWM Least Significant bits

Capture Mode: Unused

Compare Mode: Unused

PWM Mode: These bits are the two LSB s of the PWM duty cycle. The eight MSB s are found in CCPRxL.

bit 3-0: **CCPxM3:CCPxM0:** CCPx Mode Select bits

0000 = Capture/Compare/PWM off (resets CCPx module)

0100 = Capture mode, every falling edge

0101 = Capture mode, every rising edge

0110 = Capture mode, every 4th rising edge

0111 = Capture mode, every 16th rising edge

1000 = Compare mode, set output on match (CCPxIF bit is set)

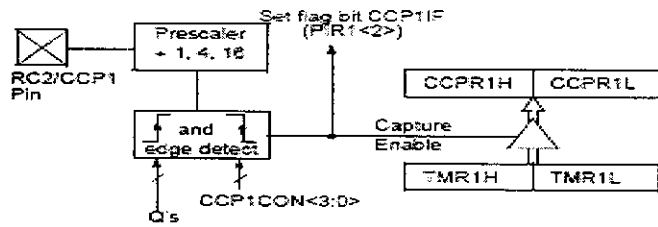
1001 = Compare mode, clear output on match (CCPxIF bit is set)

1010 = Compare mode, generate software interrupt on match (CCPxIF bit is set, CCPx pin is unaffected)

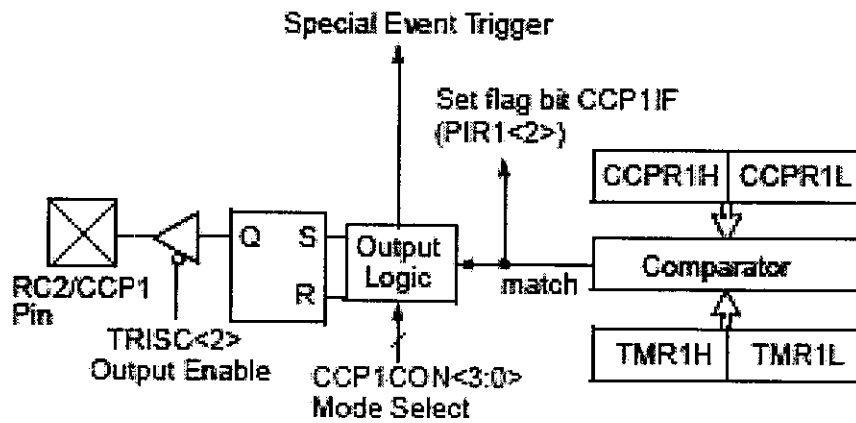
1011 = Compare mode, trigger special event (CCPxIF bit is set, CCPx pin is unaffected); CCP1 resets TMR1; CCP2 resets TMR1 and starts an A/D conversion (if A/D module is enabled)

11xx = PWM mode

**CAPTURE MODE OPERATION BLOCK DIAGRAM:**



**COMPARE MODE OPERATION BLOCK DIAGRAM:**



## N-channel enhancement mode TrenchMOS™ transistor

IRFZ44N

### GENERAL DESCRIPTION

N-channel enhancement mode standard level field-effect power transistor in a plastic envelope using 'trench' technology. The device features very low on-state resistance and has integral zener diodes giving ESD protection up to 2kV. It is intended for use in switched mode power supplies and general purpose switching applications.

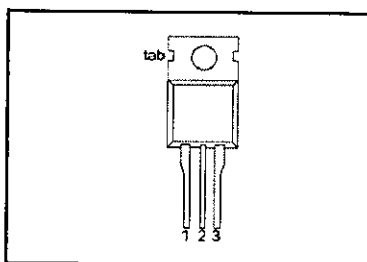
### QUICK REFERENCE DATA

SYMBOL	PARAMETER	MAX.	UNIT
$V_{DS}$	Drain-source voltage	55	V
$I_D$	Drain current (DC)	49	A
$P_{tot}$	Total power dissipation	110	W
$T_j$	Junction temperature	175	°C
$R_{DS(ON)}$	Drain-source on-state resistance $V_{GS} = 10\text{ V}$	22	mΩ

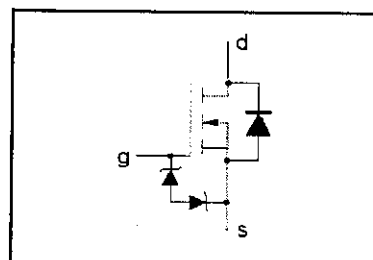
### PINNING - TO220AB

PIN	DESCRIPTION
1	gate
2	drain
3	source
tab	drain

### PIN CONFIGURATION



### SYMBOL



### LIMITING VALUES

Limiting values in accordance with the Absolute Maximum System (IEC 134)

SYMBOL	PARAMETER	CONDITIONS	MIN.	MAX.	UNIT
$V_{DS}$	Drain-source voltage	-	-	55	V
$V_{DGR}$	Drain-gate voltage	$R_{GS} = 20\text{ k}\Omega$	-	55	V
$\pm V_{GS}$	Gate-source voltage	-	-	20	V
$I_D$	Drain current (DC)	$T_{mb} = 25\text{ }^\circ\text{C}$	-	49	A
$I_D$	Drain current (DC)	$T_{mb} = 100\text{ }^\circ\text{C}$	-	35	A
$I_{DM}$	Drain current (pulse peak value)	$T_{mb} = 25\text{ }^\circ\text{C}$	-	160	A
$P_{tot}$	Total power dissipation	$T_{mb} = 25\text{ }^\circ\text{C}$	-	110	W
$T_{stg}, T_j$	Storage & operating temperature	-	-55	175	°C

### ESD LIMITING VALUE

SYMBOL	PARAMETER	CONDITIONS	MIN.	MAX.	UNIT
$V_C$	Electrostatic discharge capacitor voltage, all pins	Human body model (100 pF, 1.5 kΩ)	-	2	kV

### THERMAL RESISTANCES

SYMBOL	PARAMETER	CONDITIONS	TYP.	MAX.	UNIT
$R_{th(j-mb)}$	Thermal resistance junction to mounting base	-	-	1.4	K/W
$R_{th(j-a)}$	Thermal resistance junction to ambient	in free air	60	-	K/W

**N-channel enhancement mode  
TrenchMOS™ transistor**

IRFZ44N

**STATIC CHARACTERISTICS** $T_j = 25^\circ\text{C}$  unless otherwise specified

SYMBOL	PARAMETER	CONDITIONS	MIN.	TYP.	MAX.	UNIT
$V_{(BR)DSS}$	Drain-source breakdown voltage	$V_{GS} = 0\text{ V}; I_D = 0.25\text{ mA}; T_j = -55^\circ\text{C}$	55	-	-	V
$V_{GS(TH)}$	Gate threshold voltage	$V_{DS} = V_{GS}; I_D = 1\text{ mA}; T_j = -55^\circ\text{C}$	50	-	-	V
		$T_j = 175^\circ\text{C}$	2.0	3.0	4.0	V
		$T_j = -55^\circ\text{C}$	1.0	-	-	V
$I_{DSS}$	Zero gate voltage drain current	$V_{DS} = 55\text{ V}; V_{GS} = 0\text{ V}; T_j = 175^\circ\text{C}$	-	0.05	10	$\mu\text{A}$
$I_{GSS}$	Gate source leakage current	$V_{GS} = \pm 10\text{ V}; V_{DS} = 0\text{ V}; T_j = 175^\circ\text{C}$	-	0.04	1	$\mu\text{A}$
$\pm V_{(BR)GSS}$	Gate source breakdown voltage	$I_G = \pm 1\text{ mA}; T_j = 175^\circ\text{C}$	-	-	20	$\mu\text{A}$
$R_{DS(ON)}$	Drain-source on-state resistance	$V_{GS} = 10\text{ V}; I_D = 25\text{ A}; T_j = 175^\circ\text{C}$	16	-	-	V
			-	15	22	$\text{m}\Omega$
			-	-	42	$\text{m}\Omega$

**DYNAMIC CHARACTERISTICS** $T_{mb} = 25^\circ\text{C}$  unless otherwise specified

SYMBOL	PARAMETER	CONDITIONS	MIN.	TYP.	MAX.	UNIT
$g_s$	Forward transconductance	$V_{DS} = 25\text{ V}; I_D = 25\text{ A}$	6	-	-	S
$C_{iss}$	Input capacitance	$V_{GS} = 0\text{ V}; V_{DS} = 25\text{ V}; f = 1\text{ MHz}$	-	1350	1800	pF
$C_{oss}$	Output capacitance		-	330	400	pF
$C_{rss}$	Feedback capacitance		-	155	215	pF
$Q_g$	Total gate charge	$V_{DD} = 44\text{ V}; I_D = 50\text{ A}; V_{GS} = 10\text{ V}$	-	-	62	nC
$Q_{gs}$	Gate-source charge		-	-	15	nC
$Q_{gd}$	Gate-drain (miller) charge		-	-	26	nC
$t_{d(on)}$	Turn-on delay time	$V_{DD} = 30\text{ V}; I_D = 25\text{ A}; V_{GS} = 10\text{ V}; R_G = 10\ \Omega$	-	18	26	ns
$t_r$	Turn-on rise time		-	50	75	ns
$t_{d(off)}$	Turn-off delay time	Resistive load	-	40	50	ns
$t_f$	Turn-off fall time		-	30	40	ns
$L_d$	Internal drain inductance	Measured from contact screw on tab to centre of die	-	3.5	-	nH
$L_d$	Internal drain inductance	Measured from drain lead 6 mm from package to centre of die	-	4.5	-	nH
$L_s$	Internal source inductance	Measured from source lead 6 mm from package to source bond pad	-	7.5	-	nH

**REVERSE DIODE LIMITING VALUES AND CHARACTERISTICS** $T_j = 25^\circ\text{C}$  unless otherwise specified

SYMBOL	PARAMETER	CONDITIONS	MIN.	TYP.	MAX.	UNIT
$I_{DR}$	Continuous reverse drain current		-	-	49	A
$I_{DRM}$	Pulsed reverse drain current		-	-	160	A
$V_{SD}$	Diode forward voltage	$I_F = 25\text{ A}; V_{GS} = 0\text{ V}$	-	0.95	1.2	V
		$I_F = 40\text{ A}; V_{GS} = 0\text{ V}$	-	1.0	-	
$t_r$	Reverse recovery time	$I_F = 40\text{ A}; -di_F/dt = 100\text{ A}/\mu\text{s}; V_{GS} = -10\text{ V}; V_R = 30\text{ V}$	-	47	-	ns
$Q_r$	Reverse recovery charge		-	0.15	-	$\mu\text{C}$

# MC78XX/LM78XX

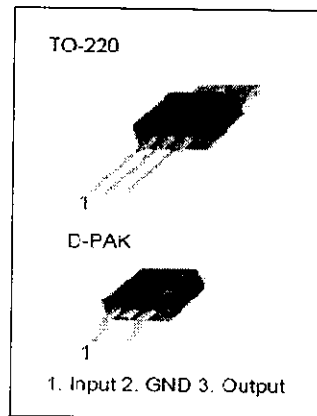
## 3-terminal 1A positive voltage regulator

### Features

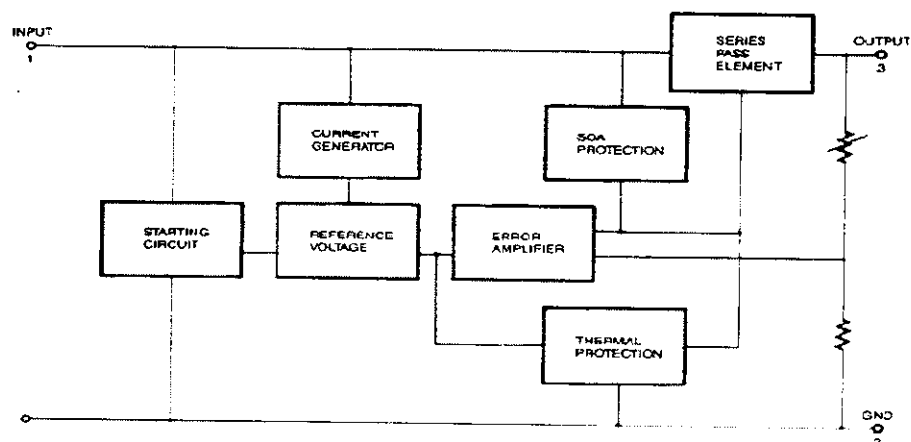
- Output Current up to 1A
- Output Voltages of 5, 6, 8, 9, 10, 11, 12, 15, 18, 24V
- Thermal Overload Protection
- Short Circuit Protection
- Output Transistor Safe Operating area Protection

### Description

The MC78XX/LM78XX series of three-terminal positive regulators are available in the TO-220/D-PAK package and with several fixed output voltages, making them useful in a wide range of applications. Each type employs internal current limiting, thermal shut-down and safe operating area protection, making it essentially indestructible. If adequate heat sinking is provided, they can deliver over 1A output current. Although designed primarily as fixed voltage regulators, these devices can be used with external components to obtain adjustable voltages and currents.



### Internal Block Diagram





## Absolute Maximum Ratings

Parameter	Symbol	LM258/LM258A	LM358/LM358A	LM2904	Unit
Supply Voltage	V <sub>CC</sub>	±16 or 32	±16 or 32	±13 or 26	V
Differential Input Voltage	V <sub>I(DIFF)</sub>	32	32	26	V
Input Voltage	V <sub>I</sub>	-0.3 to +32	-0.3 to +32	-0.3 to +26	V
Output Short Circuit to GND V <sub>CC</sub> ≤ 15V, T <sub>A</sub> = 25°C (One Amp)	-	Continuous	Continuous	Continuous	-
Operating Temperature Range	TOPR	-25 ~ +85	0 ~ +70	-40 ~ +85	°C
Storage Temperature Range	TSTG	-65 ~ +150	-65 ~ +150	-65 ~ +150	°C

## Electrical Characteristics

(V<sub>CC</sub> = 5.0V, V<sub>EE</sub> = GND, T<sub>A</sub> = 25°C, unless otherwise specified)

Parameter	Symbol	Conditions	LM258			LM358			LM2904			Unit
			Min.	Typ.	Max.	Min.	Typ.	Max.	Min.	Typ.	Max.	
Input Offset Voltage	V <sub>IO</sub>	V <sub>CM</sub> = 0V to V <sub>CC</sub> -1.5V V <sub>O(P)</sub> = 1.4V, R <sub>S</sub> = 0Ω	-	2.9	5.0	-	2.9	7.0	-	2.9	7.0	mV
Input Offset Current	I <sub>IO</sub>	-	-	3	30	-	5	50	-	5	50	nA
Input Bias Current	I <sub>BIAS</sub>	-	-	45	150	-	45	250	-	45	250	nA
Input Voltage Range	V <sub>I(R)</sub>	V <sub>CC</sub> = 30V (LM2904, V <sub>CC</sub> = 26V)	0	-	V <sub>CC</sub> -1.5	0	-	V <sub>CC</sub> -1.5	0	-	V <sub>CC</sub> -1.5	V
Supply Current	I <sub>CC</sub>	R <sub>L</sub> = ∞, V <sub>CC</sub> = 30V (LM2904, V <sub>CC</sub> = 26V)	-	0.8	2.0	-	0.8	2.0	-	0.8	2.0	mA
		R <sub>L</sub> = ∞, V <sub>CC</sub> = 5V	-	0.5	1.2	-	0.5	1.2	-	0.5	1.2	mA
Large Signal Voltage Gain	G <sub>V</sub>	V <sub>CC</sub> = 15V, R <sub>L</sub> = 2kΩ V <sub>O(P)</sub> = 1V to 11V	50	100	-	25	100	-	25	100	-	V/mV
Output Voltage Swing	V <sub>O(H)</sub>	V <sub>CC</sub> = 30V, R <sub>L</sub> = 2kΩ	26	-	-	26	-	-	22	-	-	V
		V <sub>CC</sub> = 26V for LM2904, R <sub>L</sub> = 10kΩ	27	28	-	27	28	-	23	24	-	V
	V <sub>O(L)</sub>	V <sub>CC</sub> = 5V, R <sub>L</sub> = 10kΩ	-	5	20	-	5	20	-	5	20	mV
Common-Mode Rejection Ratio	CMRR	-	70	85	-	65	80	-	50	80	-	dB
Power Supply Rejection Ratio	PSRR	-	65	100	-	65	100	-	50	100	-	dB
Channel Separation	CS	f = 1kHz to 20kHz (Note 1)	-	120	-	-	120	-	-	120	-	dB
Short Circuit to GND	I <sub>SC</sub>	-	-	40	60	-	40	60	-	40	60	mA
Output Current	I <sub>SOURCE</sub>	V <sub>I(+)</sub> = 1V, V <sub>I(-)</sub> = 0V, V <sub>CC</sub> = 15V, V <sub>O(P)</sub> = 2V	20	30	-	20	30	-	20	30	-	mA
		V <sub>I(+)</sub> = 0V, V <sub>I(-)</sub> = 1V, V <sub>CC</sub> = 15V, V <sub>O(P)</sub> = 2V	10	15	-	10	15	-	10	15	-	mA
	I <sub>SINK</sub>	V <sub>I(+)</sub> = 0V, V <sub>I(-)</sub> = 1V, V <sub>CC</sub> = 15V, V <sub>O(P)</sub> = 200mV	12	100	-	12	100	-	-	-	-	μA
Differential Input Voltage	V <sub>I(DIFF)</sub>	-	-	V <sub>CC</sub>	-	-	V <sub>CC</sub>	-	-	V <sub>CC</sub>	-	V